THE UNIVERSITY OF AUCKLAND
NEW ZEALAND

Physics 245 — Frontiers in Physics — 2020

Episode I: Lasers and Optical Frequency Combs

Dr Miro Erkintalo
Physics Department
Room 505
m.erkintalo@auckland.ac.nz
ext. 85598

Contents

1 Introduction

Lasers are used in every nook and cranny of modern society, and they play a central role in our everyday lives. They are key enablers of numerous technologies that we today take for granted, such as barcode scanners or CD players. Moreover, they are widely employed in industrial manufacturing for welding and cutting; if you buy a new car today, it was made using lasers. Internet is similarly enabled by lasers, and would simply not exist if it were not for lasers. Overall, lasers enable industries whose global annual revenues are measured in trillions of dollars. They also play a key role in basic science, and have led to numerous scientific breakthroughs over the last 57 years: they have enabled researches that have led to 28 Nobel prizes in physics and chemistry.

These lecture notes (and the associated lectures) survey basics of laser physics, focussing on two closely intertwined technologies that are today enabling breakthroughs at the frontiers of physics: ultrashort pulsed lasers and optical frequency combs. The former correspond to devices that allow for the creation of the shortest events realised by humankind, i.e., femtosecond bursts of light. The latter are enabling the most precise measurements that have ever been made; their inventors were awarded the 2005 Nobel Prize of Physics

In keeping with the spirit of Physics 245, the current lecture notes are stripped of much of the salient mathematics, and the results are "given for free". Much deeper details of the underlying mathematics and physics can be found from the following lecture notes:

More in-depth material for those interested.

- *Physics 333: Lasers and EM waves* by M. Erkintalo
- *Physics 726: Optoelectronics – Optical Frequency Combs* by M. Erkintalo

Both lecture notes can be found from the instructor's website www.miroerkintalo.com/teaching.html.

1.1 Preliminaries

In the discussion that follows, we will make extensive use of the wave-particle duality of light:

- Light corresponds to an electromagnetic wave with frequency f, angular frequency $\omega = 2\pi f$, and wavelength $\lambda = c/(nf) = 2\pi c/(n\omega)$, where n is the refractive index and c is the speed of light in vacuum.
- Light also corresponds to a stream of particles known as photons, each of which carry a quantum of energy $E = \hbar\omega$, where $\hbar = h/(2\pi)$ is the Reduced Planck constant.

1.2 Special characteristics of laser light

Lasers are devices that emit coherent light through a process of optical amplification via stimulated emission of radiation. Their usefulness originates from the many attractive and unique characteristics possessed by laser light compared to other forms of light (generated by e.g. light bulbs or stars). These characteristics include:

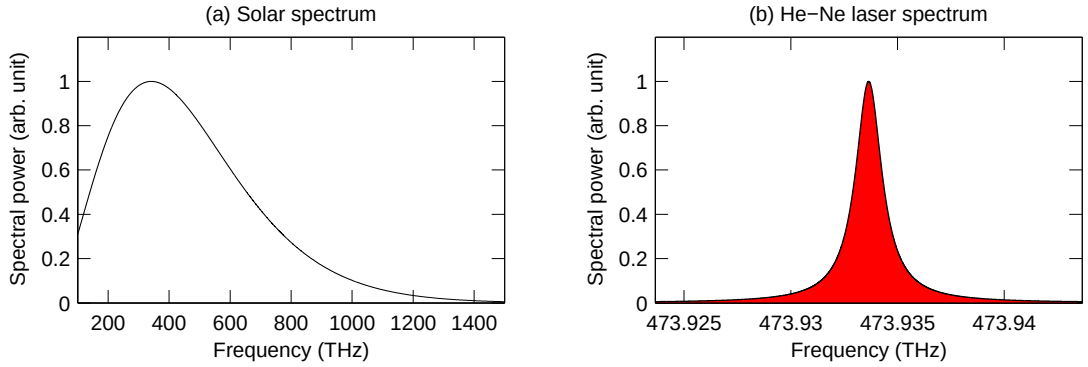

Figure 1: Comparison between spectral intensities of light emanating from (a) the Sun and (b) a He-Ne laser. Note the different x-axis scales. (a) Corresponds to the spectrum of a black body at $T = 5800$ K.

1. **Monochromaticity:** Lasers can produce very pure colours, i.e., electromagnetic waves with a very precise frequency. Light emitted by the sun or a light bulb is white, containing frequencies spanning hundreds of THz. In contrast, laser light can have a bandwidth as small as 1 Hz [see Fig. 1].

2. **Directionality:** While most light sources emit light in all directions, lasers can create narrow unidirectional beams that diffract (i.e., broaden) extremely slowly. In radians, the divergence (half-)angle of a diffraction-limited laser beam is:
$$\theta \approx \frac{\lambda}{\pi w_0}, \tag{1.1}$$
where λ is wavelength and w_0 is the initial width of the beam. For a typical red laser with $\lambda = 633$ nm and spot size $w_0 = 5$ mm, one obtains $\theta \approx 4 \times 10^{-5}$ rad. One can easily confirm that a propagation length of more than 120 metres is needed for the spot size to double.

3. **Brightness/intensity:** Because of their small beam size and ability to be focussed to very small spots, lasers can concentrate light energy very tightly, resulting in extreme brightness and high intensities[1].

   Example.
   The total solar intensity *on earth* is
   $$\frac{P_{\text{sun}}}{A} \approx 1380 \frac{\text{W}}{\text{m}^2}, \tag{1.2}$$
   while the intensity of a 1 mW laser focussed to a 80 μm (radius) spot is
   $$\frac{P_{\text{laser}}}{A} \approx 50000 \frac{\text{W}}{\text{m}^2}. \tag{1.3}$$

4. **Short durations:** Lasers can create very short bursts of light, i.e. pulses, with durations well below 100 fs (10^{-15} s) [see Fig. 2]. In fact, such ultrashort laser pulses correspond to the shortest events created by humankind. Because of their short duration, ultrashort pulses can also possess extremely large peak powers.

[1] Intensity is the rate of energy transfer per unit area, i.e., power per area.

Example.
Commercial Ti:Sapphire lasers can readily produce $\Delta\tau = 100$ fs pulses at a repetition rate $f_{\text{rep}} = 80$ MHz (i.e., 80 million pulses per second) with average power $P_{\text{avg}} = 1$ W. This corresponds to a peak power (per pulse) of $P_{\text{peak}} = 125$ kW. Assuming a 5 mm beam spot, the corresponding peak intensity is about

$$\frac{P_{\text{peak}}}{A} \approx 6400 \, \frac{\text{MW}}{\text{m}^2}. \tag{1.4}$$

This is 100 times larger than the total solar intensity on the surface of the sun.

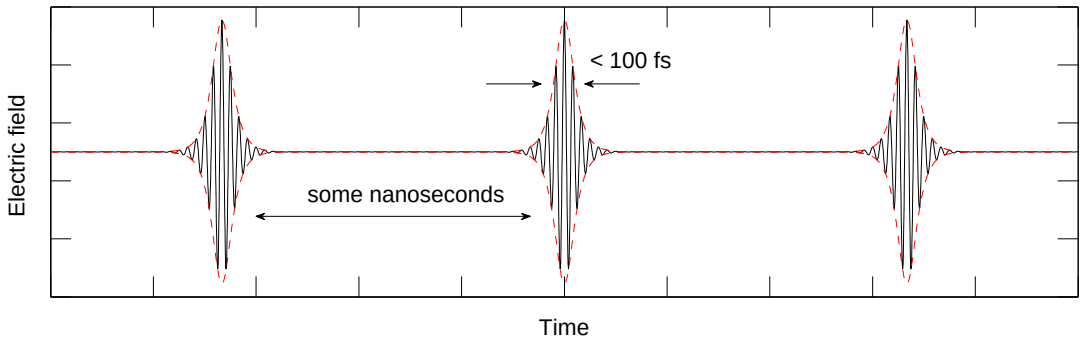

Figure 2: Schematic illustration of the electric field of an EM wave corresponding to a train of ultrashort pulses. Black curve illustrates the electric field, while the red dashed curve depicts the *envelope*.

All of these distinctive characteristics ensue from the fact that laser light originates from a fundamentally different physical process than any other form of light. Specifically, whereas light generated in stars (e.g., the Sun) or heated filaments (e.g., light bulbs) arise from *spontaneous* emission of photons by excited atoms/molecules, laser light originates from a process known as *stimulated* emission. Hence the name: **L**ight **A**mplification by **S**timulated **E**mission of **R**adiation. As we shall see, spontaneous emission results in the generation of photons with random traits (phase, frequency, polarisation, direction), while stimulated emission results in the generation of photons with identical characteristics. It should be evident that this fact (namely the creation of photons with identical phase, frequency, direction) is sufficient to explain the unique characteristics of laser light listed above.

1.3 Ultrashort history of lasers

The story of the laser arguably begins with the quantum hypothesis put forward by Max Planck around 1900. In particular, he proposed that atoms can only absorb and emit radiation in discrete quanta. As we shall see below, this behaviour is paramount for laser operation.

The concept of stimulated emission, which underpins laser operation, was hypothesised in 1917 by Albert Einstein. Classical electromagnetism could only account for the processes of absorption and spontaneous emission, which had left stimulated emission undiscovered. Einstein considered an atom in thermal equilibrium with a black body radiation field, and showed that Plank's law (of black body radiation) could be re-derived

only if the atom could undergo the hypothesised process of stimulated emission (in addition to absorption and spontaneous emission).

Stimulated emission was first realised in the laboratory not in the optical but in the microwave domain. The idea for a device utilising stimulated emission to realise coherent sources of microwave radiation (MASER: microwave amplification by stimulated emission of radiation) was first conceived (independently) by Joseph Weber, Charles Townes, Nikolay Basov, and Aleksandr Prokhorov around 1950. The first laboratory demonstration of a maser was reported in 1954 by Townes, together with J. P. Gordon and H. J. Zeiger.

Conceptually, lasers can be considered as masers operating in the optical domain. Their practical construction is, however, technologically different. In 1957, Gordon Gould conceived the idea of building a laser using an open-sided Fabry-Perot resonator. Similar ideas were simultaneously pursued by Townes together with A. Schawlow.

The first actual laser was built and demonstrated by Theodore Maiman in 1960. Using a ruby crystal pumped by photographic flash lamps, he realised pulsed laser operation with a wavelength of 694.3 nm (red). From there onwards, numerous different lasers and laser technologies were quickly developed.

In 1964, Townes Basov, and Prokhorov won the Nobel Prize in Physics "for fundamental work in the field of quantum electronics, which has led to the construction of oscillators and amplifiers based on the maser-laser principle."

2 Basics of laser physics

This Section summarises the basics of laser physics. We first describe the necessary components that make up almost all lasers demonstrated to date, and then describe the physics underlying optical amplification via stimulated emission of radiation. Subsequently, we briefly describe the role of optical resonators, before moving on to explain the generation of ultra-short pulses via a process known as mode-locking.

2.1 Basic laser construction

Virtually all lasers include three key components which play crucial roles for enabling laser operation. These are highlighted in Fig. 3, where we show a schematic illustration of a generic laser design.

Key laser components

1. **Active medium:** provides light amplification via *stimulated emission of radiation.* More light (i.e., photons) come out of the active medium than what go in.
2. **Pumping:** provides energy needed for light amplification in the active medium. Each photon carries energy, and we must inject energy into the active medium to be able to create more photons.
3. **Resonator (or cavity):** allows light to travel through the active medium many times, thus enabling strong light amplification. The simplest embodiment of an optical resonator consists of two mirrors facing each other, but other configurations are also often encountered (e.g. numerous mirrors or an optical fibre ring resonator).

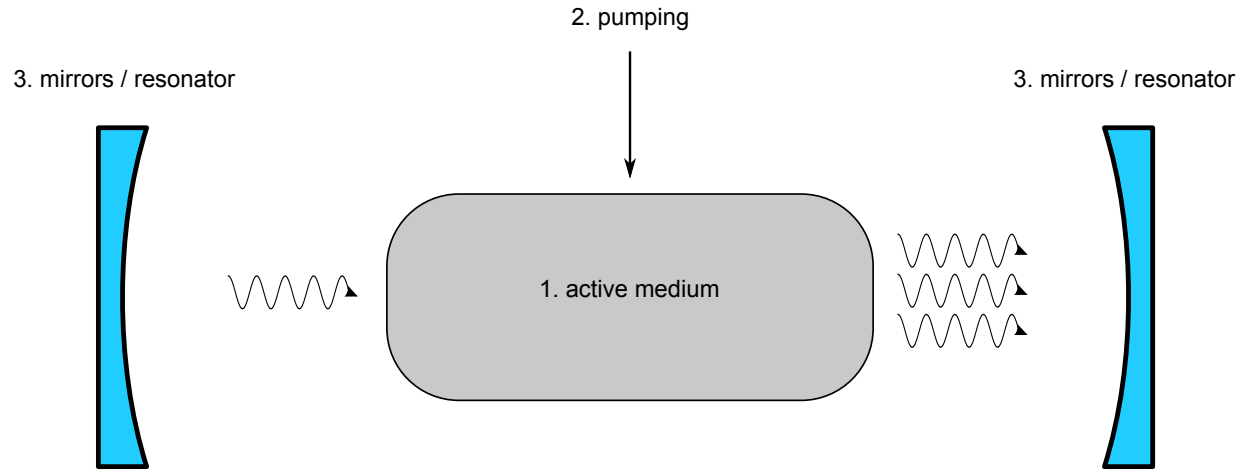

Figure 3: Schematic illustration of a generic laser construction. Three key components are highlighted: active medium, pumping, and a resonator (in this embodiment formed by two mirrors). Also illustrated is optical amplification in the active medium.

2.2 Light-matter interactions

Laser light is generated through a quantum mechanical process known as stimulated emission. Through this process, light entering an active medium can be **amplified**, i.e., more light can come out than what goes in. The simplest way to explain how such amplification takes place is to consider how photons (particles of light) interact with individual atoms (or ions or molecules) that make up the active medium. Here, we accept it as an experimental fact that the energies of atoms (or ions or molecules) are quantised, i.e., an atom can only occupy some discrete energy levels.

There are three mechanisms through which light can mediate transitions between atomic energy levels, as shown in Fig. 4.

Mechanisms of light-matter interaction

1. **Spontaneous emission:** an atom in an excited state spontaneously decays to a lower energy state, while simultaneously emitting a photon with energy $\hbar\omega_{21} = E_2 - E_1$, where E_2 and $E_1 < E_2$ are the energies of the atomic states. The emitted photon has random phase, is emitted in a random direction, and at a random time. Spontaneous emission is behind almost all forms of light, including sun light and artificial lights. (The only real exception is laser light.) It is so prevalent, that it has several names. These include luminescence, fluorescence, and phosphorescence.

2. **Absorption:** an atom in the lower level can be excited to an upper level by the absorption (annihilation) of a photon with energy $\hbar\omega_{21} = E_2 - E_1$.

3. **Stimulated emission:** a photon with energy $\hbar\omega_{21} = E_2 - E_1$ can *stimulate* an atom in the upper level to decay to the lower level state by the emission of a second photon of energy $\hbar\omega_{21}$. The stimulated photon has the exact same frequency, direction, phase, and polarisation of the incident photon. This "cloning" of the initial photon underpins the special characteristics of laser light.

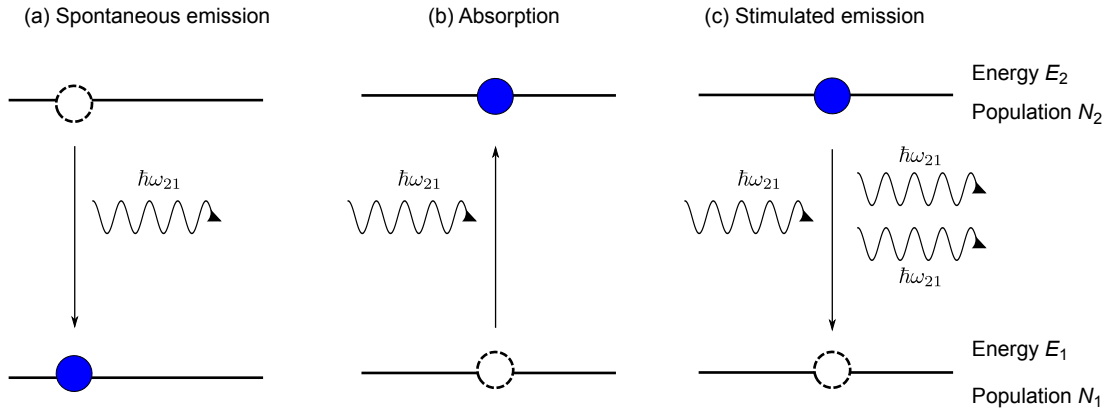

Figure 4: Schematic illustration of the three different mechanisms through which light can mediate transitions between atomic energy levels: (a) spontaneous emission, (b) absorption, and (c) stimulated emission. Here, E_2 and E_1 correspond to the energies of the upper and lower states, N_2 and N_1 are the corresponding populations (i.e., the number of atoms on each state), and ω_{21} is the transition (angular) frequency.

2.3 Population inversion

Let us now consider a bunch of identical photons launched into an active medium. As explained above, each absorption event annihilates one photon, whilst each stimulated emission event creates one new photon. (We are not interested in spontaneous emission, as those photons are generated with random characteristics.) Thus, to obtain net amplification, we need more stimulated emission events than absorption events. It turns out that *the probability of stimulated emission per atom is the same as the probability of absorption per atom*. This means that, if a single photon interacts with two atoms, one of which is excited and the other one which is not, there is a 50/50 probability that the photon will be absorbed or cloned through stimulated emission. However, these 50/50 odds only apply when the number of excited atoms equals the number of atoms in the ground state. In contrast, if there are more (less) atoms in the upper state than in the lower state, the overall probability of stimulated emission will be greater (smaller) than absorption. One finds that optical amplification can occur only when

$$N_2 > N_1, \tag{2.1}$$

where N_2 and N_1 are the number of atoms in the upper and lower states, respectively. In other words,

> A necessary condition for light amplification by stimulated emission of radiation is that the population on the upper energy is larger than the population on the lower energy level. This situation is known as **population inversion**.

2.3.1 The very unnatural nature of population inversion

Population inversion is a necessary condition for optical amplification. It corresponds to a very unusual situation, and one which does not spontaneously occur in nature. To highlight this, consider a bunch of atoms in thermal equilibrium. It is known from statistical physics that the ratio of atomic populations at two energy

levels E_2 and $E_1 < E_2$ obey Boltzmann statistics. Specifically, we have

$$\frac{N_2}{N_1} = e^{-\frac{E_2 - E_1}{kT}} = e^{-\frac{\hbar\omega_{21}}{kT}}. \tag{2.2}$$

We see immediately that, for all temperatures $T > 0$, $N_2 < N_1$, and so population inversion cannot occur in thermal equilibrium. The example below highlights the severity of the problem.

Example. Consider a transition corresponding to red laser light, with a wavelength of $\lambda = 2\pi c/\omega_{21} = 633$ nm, where c is the speed of light. At room temperature ($T = 293$ K), the ratios of the populations on the upper and lower energy levels of the laser transition in thermal equilibrium is:

$$\frac{N_2}{N_1} = e^{-\frac{\hbar\omega_{21}}{kT}} \approx 2 \times 10^{-34}. \tag{2.3}$$

That is 34 orders of magnitude away from population inversion ($N_2 > N_1$).

2.3.2 Pumping

To reach population inversion, we must move away from thermal equilibrium. Specifically, we must externally inject energy into the system, so as to force atoms to occupy the upper level. This is achieved by the second key component of our basic laser design: **pumping**.

Pumping is typically achieved either electronically or optically. Electronic pumping is mostly used for gas lasers and semiconductor lasers, and is achieved by passing an electric current through the medium. For example, in semiconductor lasers this results in direct addition of electrons in the conducting band, from which they can transition to the valence band via stimulated emission. In gas lasers, the current causes electrons to collide, with gas atoms, which leads to their excitation.

In optical pumping, atoms are excited directly through absorption: the frequency of **a pump light source** is tuned to match with a transition, and absorption lifts atoms from the lower state to the upper state [see Fig. 5].

3 Resonators and mode-locking

In the discussion above, we assumed the photon energies to be exactly equal to the atomic transition energy, i.e., $\hbar\omega_{21} = E_2 - E_1$. But of course, in practice, even photons whose frequencies are not exactly equal to the transition frequency [$\omega_{21} = (E_2 - E_1)/\hbar$] can mediate transitions between energy levels (they just do so less efficiently). This can be understood simply by noting that the atomic energy levels themselves are not infinitely sharp, but rather, they have some finite "width". As a consequence, the active medium tends to amplify a whole range of frequencies within some finite **gain bandwidth**. Accordingly, in steady-state laser operation, the frequency *spectrum* of the emitted light does not correspond to a single infinitely sharp line, but can rather encompass a range of frequencies determined by the gain spectrum.

In addition to the gain spectrum (i.e., the range of frequencies amplified in the active medium), the precise wavelengths that a laser can emit is influenced by the **laser cavity** (synonym for laser resonator). For a cavity comprising of two mirrors, the wavelengths must be such that the two electromagnetic waves propagating in

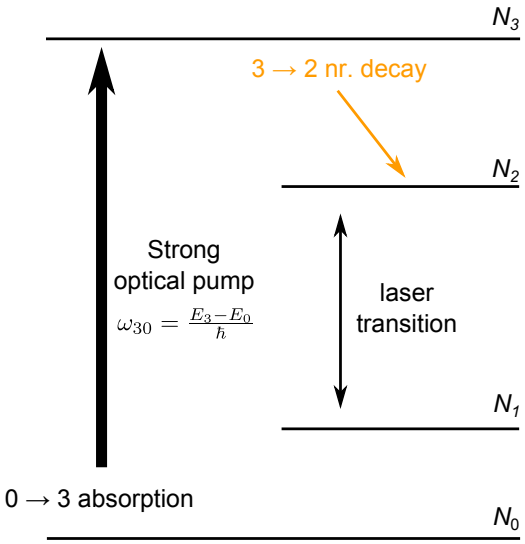

Figure 5: Schematic illustration of optical pumping. The frequency of a strong pump light source (e.g. another laser) is tuned to match with the transition ω_{30}. Atoms from level 0 are then lifted to the state 3 via absorption. In this particular example, the atoms then decay to the upper laser level non-radiatively.

opposite directions inside the cavity form standing waves. It turns out that the condition for standing waves to form inside such a laser cavity is exactly the same as the condition for standing waves to form on a string. Specifically, **the resonator must fit an integer number of half-wavelengths** [see Fig. 6]. More generally, for arbitrary resonators (including ring resonators) one finds that the laser wavelength must be such that **an integer number of wavelengths fits within one full round trip**. Thus, a laser can only emit light with the following wavelengths and frequencies (in steady-state):

$$\lambda_m = \frac{L_{\text{tot}}}{m} \tag{3.1}$$

$$f_m = \frac{c}{nL_{\text{tot}}} m, \tag{3.2}$$

where L_{tot} is the total round trip length of the resonator (for just two mirrors separated by a length L, we have $L_{\text{tot}} = 2L$), n is the refractive index inside the resonator, and m is an integer. The allowed frequencies f_m are known as the **resonance frequencies** of the cavity, and the electromagnetic waves with these frequencies are known as **longitudinal modes** of the cavity. Because optical frequencies are very large, and resonators have macroscopic dimensions, the integer m is typically very large. For example, considering a Helium-Neon laser with $\lambda = 633\ \text{m}$ and a typical cavity length of $L = 0.5\ \text{m}$, we obtain $m \approx 1.6 \times 10^6$.

It should be clear that there can be infinitely many resonance frequencies f_m. Furthermore, the spacing of neighbouring resonance frequencies is constant. This constant is known as the cavity **free-spectral range** (FSR), and it describes the frequency separation of the longitudinal modes. The FSR of an arbitrary cavity is

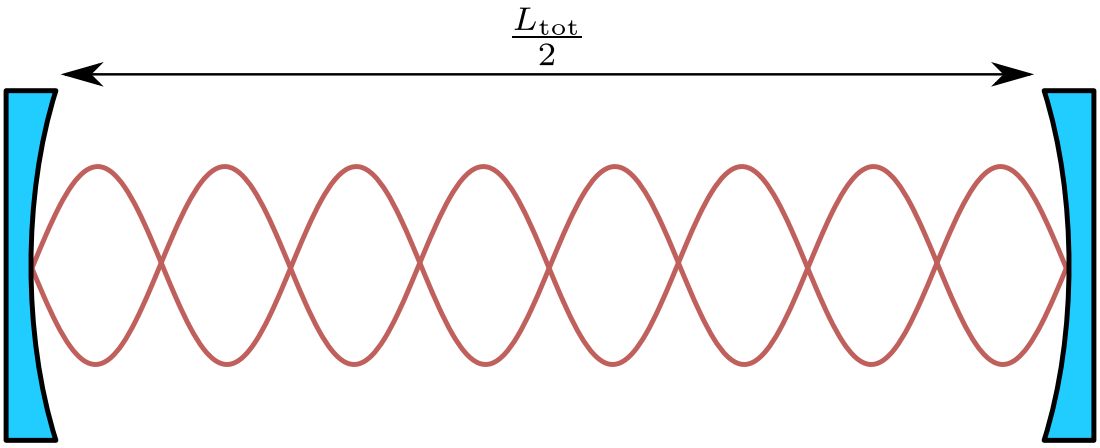

Figure 6: The wavelengths emitted by the laser are set by a resonance condition: the cavity must fit an integer number of wavelengths within one full round trip.

given by

$$\mathrm{FSR} = f_{m+1} - f_m = \frac{c}{nL_{\mathrm{tot}}}. \tag{3.3}$$

From this expression, we also see that $\mathrm{FSR} = t_{\mathrm{R}}^{-1}$, where $t_{\mathrm{R}} = nL_{\mathrm{tot}}/c$ is the time that it takes for light to complete one full round trip in the resonator.

Example.

Commercial Ti:Sapphire lasers typically come with a cavity whose total length $L_{\mathrm{tot}} \approx 3.6\ \mathrm{m}$. Therefore the cavity FSR $\approx 82\ \mathrm{MHz}$ and it takes light approximately $t_{\mathrm{R}} = \mathrm{FSR}^{-1} = 12\ \mathrm{ns}$ to complete one full round trip.

3.1 Multimode operation

Steady-state lasing can in principle occur at any of the longitudinal modes. But of course, in practice lasing only occurs at those longitudinal modes that experience net amplification over one full round trip. In general, it is possible that several longitudinal modes fall within the gain bandwidth [see Fig. 7(a)]. Depending on the precise mechanism that gives rise to the finite gain bandwidth, it is possible that all of the longitudinal modes experiencing net amplification oscillate in steady-state, giving rise to an emission spectrum similar to that shown in Fig. 7(b). In contrast, for some other "gain broadening" mechanisms, only a single longitudinal mode will persist in steady-state[2].

[2] Active media can in general be divided into two categories, depending on the mechanisms that give rise to a finite gain bandwidth. Specifically, a laser transition can be either "homogeneously" or "inhomogeneously" broadened. Typically, we find that homogeneously broadened active media always only oscillate on a single longitudinal mode, whilst "inhomogeneous" broadening can give rise to multimode operation

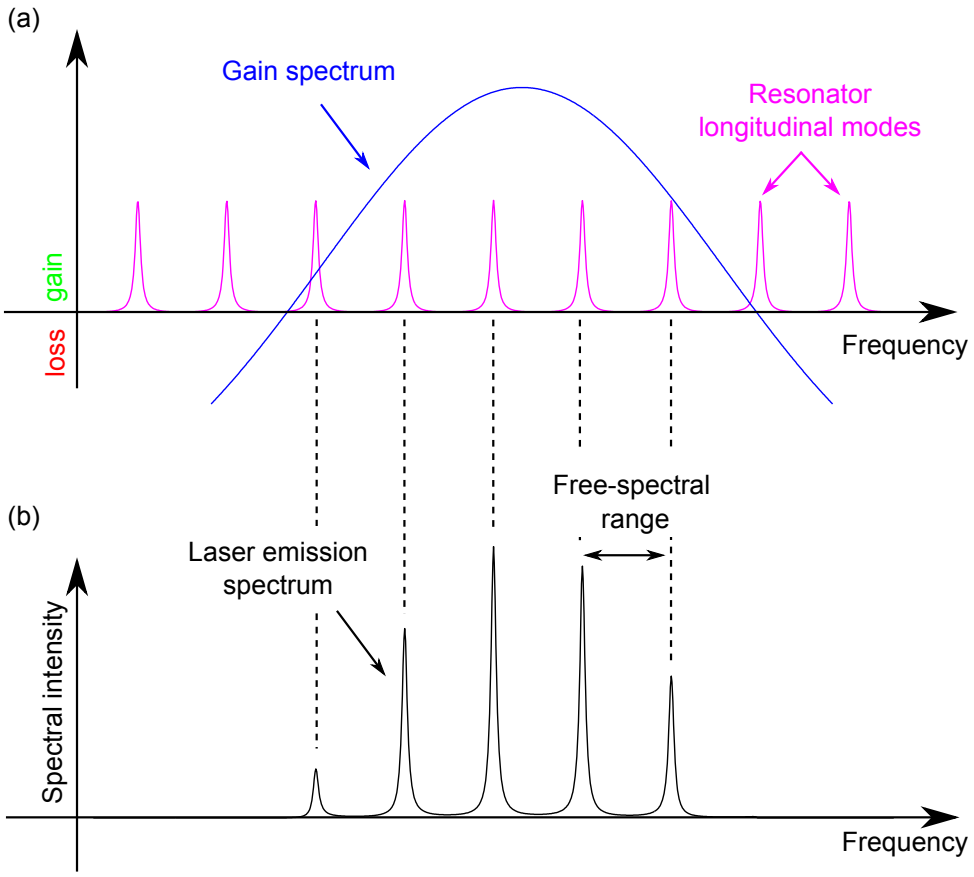

Figure 7: Schematic illustration of multimode operation. (a) Several longitudinal modes fall inside the gain bandwidth, and will hence be amplified. In steady-state, this may lead to multimode operation, where all the amplified longitudinal modes oscillate simultaneously. (b) Multimode output spectrum.

When a laser is simultaneously emitting several longitudinal modes, it is said to be in **multimode** operation. Such operation is typically unwanted, as it destroys the nice monochromaticity that underpins many of the most interesting laser applications. Furthermore, all of the individual longitudinal modes typically grow and oscillate independently from one another. As a consequence, the EM waves corresponding to different resonance frequencies have arbitrary phase relationships: in the time domain, their interference gives rise to a chaotic intensity distribution, as shown in Fig. 8(a). This is not very desirable for any application.

Example.

Consider again a commercial Ti:Sapphire lasers, with a cavity FSR ≈ 82 MHz. The gain bandwidth of a typical Ti:Sapphire device is $\Delta f \approx 15$ THz. This implies that there can be $N = \Delta f/\text{FSR} \approx 183,000$ longitudinal modes oscillating at the same time! Talk about multimode!

3.2 Mode-locking

Consider a multimode laser emitting N longitudinal modes. The complex electric field of the EM wave emitted by the laser can be written as a superposition of waves with different frequencies:

$$E(t) \approx \sum_{m=0}^{N-1} E_{0m} e^{i(\omega_0 + m2\pi\text{FSR})t + i\phi_m}, \tag{3.4}$$

where E_{0m} and ϕ_m describe the amplitudes and phases of the EM waves corresponding to the different longitudinal modes. If the phases ϕ_m are random, the temporal intensity profile $I(t) = |E|^2$ is chaotic, as shown in Fig. 8(a). However, if the phases are not random, but for example assume the same value (e.g. $\phi_m = 0$ for all m), the intensity profile is very different. Indeed, as shown in Fig. 8(b), in this case we find that the time domain laser output corresponds to a periodic train of pulses, i.e., bursts of laser light surrounded by long regions of zero intensity. The temporal separation of the pulses is found to be exactly equal to the cavity round trip time $t_\text{R} = \text{FSR}^{-1}$, and the duration of a single pulse is found to be inversely proportional to the gain bandwidth:

$$\Delta\tau \approx \frac{1}{\Delta f}. \tag{3.5}$$

When the longitudinal modes of a multimode laser oscillate in phase, we say that the laser is **mode-locked**. We can interpret the formation of the ensuing pulse train in two different ways. First, we can imagine a single laser pulse that is bouncing back and forth between the cavity mirrors; the output pulse train emerges as some part of the intracavity pulse is ejected out from the cavity each round trip. This interpretation very naturally explains the fact that the temporal spacing between the pulses is equal to the cavity round trip time: it takes the laser pulse one round trip time to complete on round trip. In this context, we often talk about the **repetition rate** f_rep of a mode-locked laser, i.e., the number of pulses emitted per second (f_rep has units of Hz). It should be clear that $f_\text{rep} = t_\text{R}^{-1} = \text{FSR}$. The second interpretation is that the pulses arise precisely when all the longitudinal modes interfere constructively. In contrast, at any other times, the modes interfere destructively, resulting in negligible intensity.

Mode-locked lasers are able to generate ultra-short pulses with durations as short as a few femtoseconds ($1\text{ fs} = 1 \times 10^{-15}\text{ s}$). These correspond to the shortest events created by humankind, and they have enabled a plethora of breakthroughs across the natural sciences. In particular, they have enabled scientists to explore events that occur in nature at femtosecond timescales, including motion of atoms during chemical reactions. (Mode-locked lasers underpin the field of femtochemistry, whose pioneer Ahmed Zewali won the Nobel Prize in chemistry in 1999.) Furthermore, in a mode-locked laser pulse, light energy is concentrated to a very short period of time. This implies that the pulses can reach extremely high peak powers (recall that $P = E/t$). It is not unconventional that the peak power of a mode-locked laser pulse exceeds the power of a nuclear power plant. Of course, the power plant is on continuously, whilst a mode-locked laser pulse only lasts for some femtoseconds. Finally, it is worth noting that very recently researchers have been able to generate laser pulses in the attosecond domain. Such pulses are short enough to probe for the motion of electrons in atoms, paving the way for an entirely new field of *attophysics*.

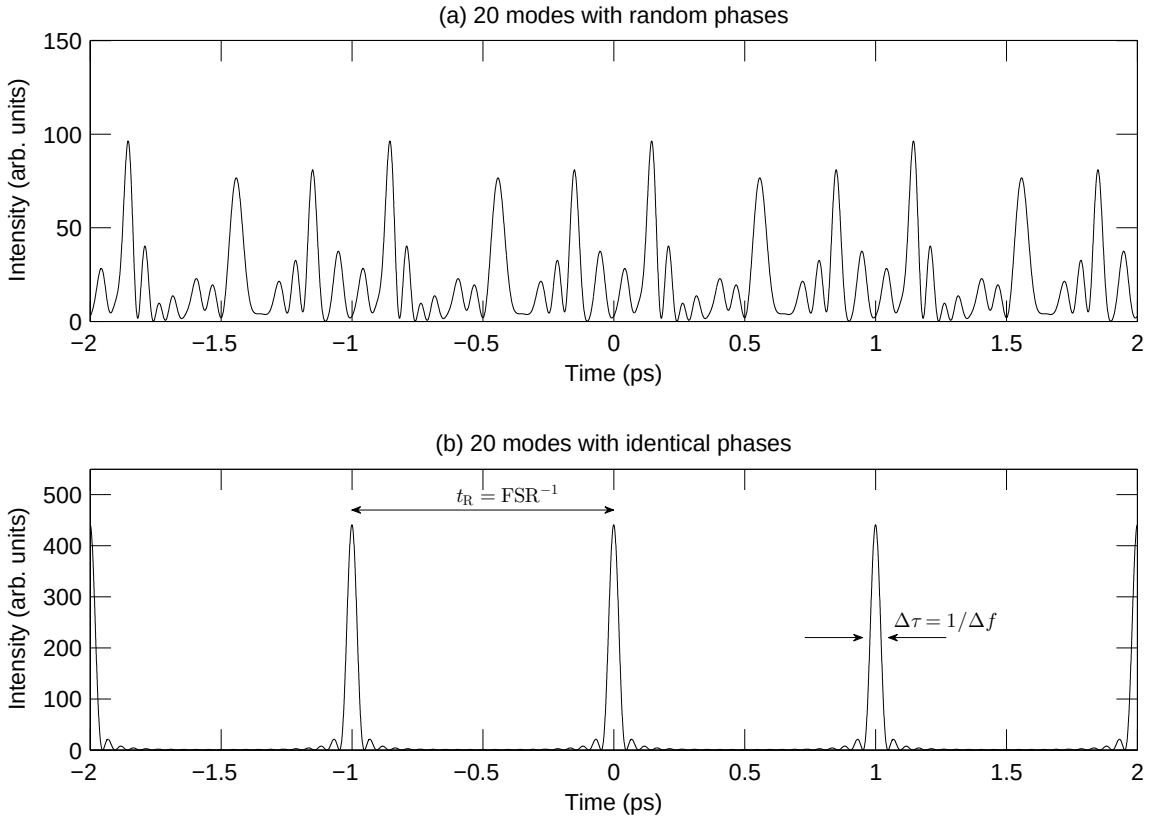

Figure 8: Temporal intensity profile corresponding to the superposition of 20 longitudinal modes with (a) random and (b) identical phases.

Example.

Let us consider once again a commercial Ti:Sapphire lasers, with a cavity FSR ≈ 82 MHz and a gain bandwidth of $\Delta f \approx 15$ THz. When mode-locked, the laser can generate 82 million pulses per second ($t_{\mathrm{R}} = 12.5$ ns), each of which has a duration of $\Delta\tau \approx 1/\Delta f \approx 67$ fs. Furthermore, under typical operating conditions, the average power emitted by such a laser is $P_{\mathrm{avg}} \approx 2$ W. This means that the individual pulses carry an energy of $E_{\mathrm{p}} \approx 24$ nJ and have a peak power of $P_{\mathrm{p}} \approx 350$ kW.

4 Introduction to frequency metrology

Metrology is the science of measurement, and so any measurement of any physical quantity belongs to the field of metrology. For decades, scientists have aimed at improving the precision of their measurements. Incidentally, *time* (and frequency) can be measured much more precisely than any other quantity. This is because measuring time is ultimately achieved by counting the cycles of a fixed frequency oscillator such as a pendulum (grandfather clock) or the oscillations of radiation corresponding to the transition between the two hyperfine

levels of the ground state of the caesium 133 atom (definition of the second). The job of a clock is to follow the passage of time by counting the "ticks" of an oscillator. Counting, on the other hand, is by nature a *digital operation* and thus immune to many sources of noise.

The ultimate precision in any time and frequency measurement is limited by the precision of the reference clock used to make the measurement. For example, if the period of the clock is known with a precision of σ, such that $\tau_{\text{per}} = \tau_0 \pm \sigma$, a measurement of time achieved by counting N cycles of the clock is $t = N\tau_{\text{per}} = N\tau_0 \pm N\sigma$. Thus, it should be clear that by improving the precision of the clock, i.e., by reducing the error σ, we can improve the absolute precision of time (and frequency) measurements.

To obtain a very precise clock, we need an oscillator whose period τ_{per} can be measured very accurately. In a perfect world, the precision with which the period of an arbitrary fixed-frequency oscillator can be measured can be increased without a limit, simply by increasing the measurement duration and counting an increased number of cycles. The improved precision then simply stems from averaging:

$$\tau_{\text{per}} = \frac{t_N}{N} \pm \frac{\sigma}{\sqrt{N}}, \tag{4.1}$$

where N is the number of cycles counted and t_N the time measured. As $N \to \infty$, the error tends to zero. However, this approach assumes that the period remains exactly constant from the beginning of the measurement to the end. Real oscillators unfortunately do not satisfy this property: in a realistic laboratory environment, the longer the measurement the more uncertain the phase of the oscillation will be owing to different sources of noise (temperature fluctuations, mechanical stress etc.). The solution is to use an oscillator with a very short period (large frequency), such that a very large number of cycles N can be counted before noise influences the oscillation.

The frequency of the Cs hyperfine transition underlying the definition of the second is 9.1 GHz. The most precise clocks (commercially) available to day are based on that transition: state-of-the-art atomic fountain clocks can achieve an uncertainty of 2.6×10^{-16}, implying they will not gain or lose a second in 138 million years. However, following the ideas outlined above, an oscillator with a larger frequency could allow us to build even better clocks. Such larger frequencies are readily available in the optical domain (wavelength of $\lambda = 1000$ nm is equivalent to a frequency $f = c/\lambda \sim 300$ THz where c is the speed of light). As a consequence, the precision of time and frequency measurements can be elevated to the next level by translating standards from the current radio domain into optical frequencies. The ultimate fractional uncertainty of time and frequency measurements based on optical atomic transitions is of the order of one part in a quintillion (10^{18}). The problem to solve is: **how to measure optical frequencies accurately**. Indeed, measuring radio frequencies (RF), such as 9.1 GHz, precisely is an easy task in electronics. Precision measurements of optical frequencies is, however, somewhat more challenging.

Joys of measuring optical frequencies

- **Optical atomic clocks**
  - $\Rightarrow$ Precision of one part in a quintillion for your everyday TV synchronization and global positioning system needs.
  - $\Rightarrow$ Eventual redefinition of the second.

- **Calibration of astronomical spectrographs**

  ⇒ For the measurement of small Doppler shifts of stars in order to reveal extra-solar planets.

- **Precision spectroscopy of hydrogen**

  ⇒ Precision tests of quantum electrodynamics (QED).

  ⇒ Precision measurement of fundamental constants.

  ⇒ Time-dependence of fundamental constants.

4.1 Difficulties in measuring optical frequencies

Optical frequencies are of the order of hundreds of terahertz. This means that the electric field of an optical electromagnetic wave completes more than 100 million million oscillations per second ($\tau_{\mathrm{per}} = 1/f$). No electronic devices exist that could directly count these oscillations and thus measure the frequency. State-of-the-art photodetectors and oscilloscopes are limited to sub-100 GHz bandwidths, and are thus incapable of resolving the oscillations of an optical electric field. The precision of interferometric wavelength measurements is limited to a precision of a few parts in 10^{10} owing to unavoidable wavefront distortions[3]. Unfortunately this is simply not precise enough.

In practice, optical signals are measured using the photoelectric effect in semiconductors. In particular, absorbed photons excite electrons in the conduction band, giving rise to a measurable electric **photocurrent**. Mathematically, the photocurrent is proportional to the absolute value squared of the complex electric field. Thus, a monochromatic electric field $E(t) = E_0 \exp(i\omega t)$ will give rise to a photocurrent of

$$i(t) \propto |E(t)|^2 = |E_0|^2. \tag{4.2}$$

In other words, a monochromatic optical field is (photo)detected as a flat line [see Fig. 9(a)]: the detector is unable to resolve the fast oscillations of the electric field, thus preventing precise measurements of the optical frequency. It is noteworthy that, if the electric field is associated with some **slowly varying envelope**, then that envelope can be detected provided that the envelope's temporal features are longer than the photodetector's impulse response (typically > 10 ps). Thus, a photodetector can detect pulses of light with durations measured in tens of picoseconds [see Fig. 9(b)], but cannot fully resolve e.g. femtosecond pulses generated by a mode-locked laser.

To summarise, photodetectors cannot resolve the individual oscillations of electric fields corresponding to optical electromagnetic waves. They can only resolve "slowly" varying temporal envelopes, and even those only if the temporal features exceed 10 ps.

4.2 Way around: beat note

Although **absolute** optical frequencies cannot be measured using conventional electronic techniques, frequency **differences** can, provided they are sufficiently small. Assume you superimpose two laser beams with different

[3] here it is yet again worth noting that nothing can be measured as accurately as frequency

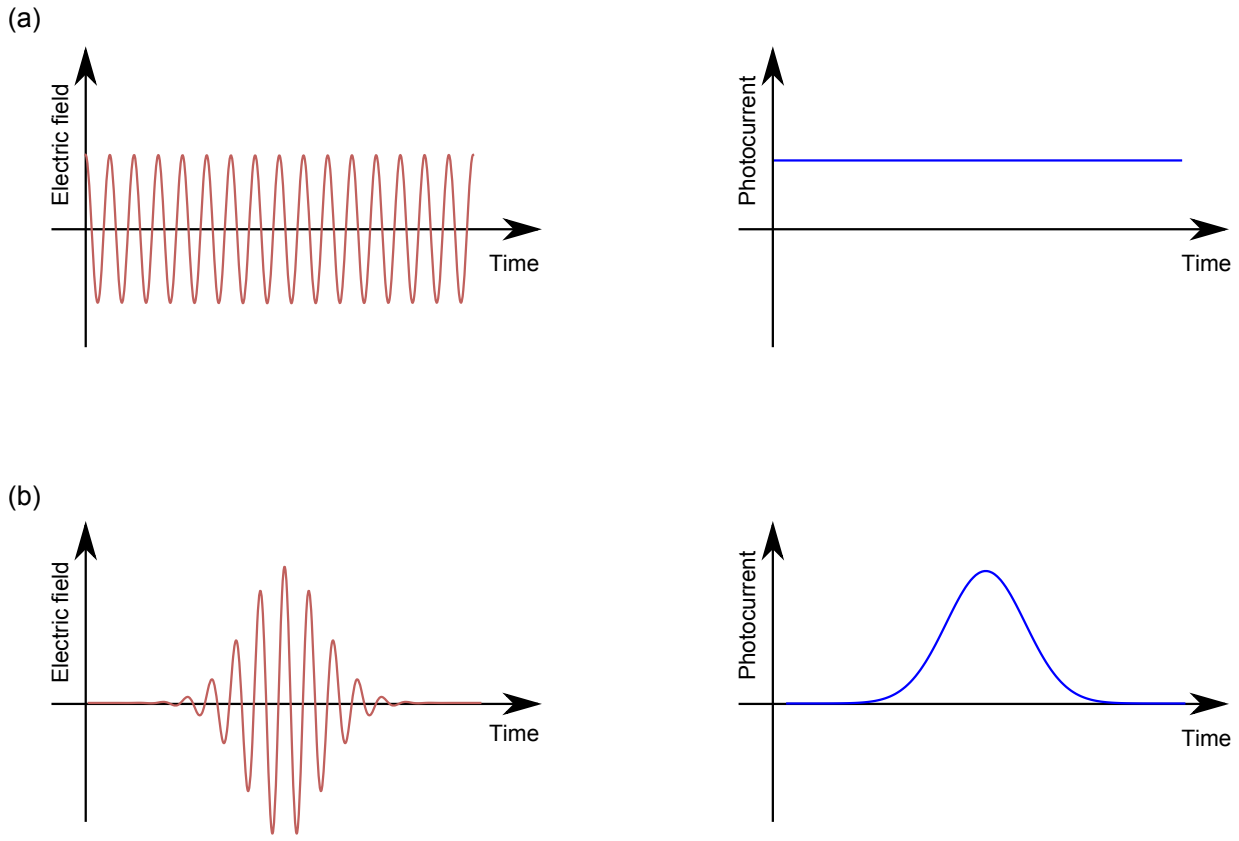

Figure 9: Photodetection does not resolve the individual oscillations of optical electric fields, but rather measures the oscillation amplitude (or light intensity). (a) A monochromatic EM wave has a constant amplitude (intensity), and is hence detected as a straight line. (b) When a burst (pulse) of light is photodetected, only the envelope (intensity) of the pulse is observed.

frequencies f_{u} and f_{r}, where f_{u} is unknown and f_{r} is a precisely known reference frequency, on a photodetector. The time-varying complex electric field at the detector can be written as

$$E(t) = E_{\mathrm{u}}(t) + E_{\mathrm{r}}(t) = E_{0\mathrm{u}}e^{i\omega_{\mathrm{u}}t} + E_{0\mathrm{r}}e^{i\omega_{\mathrm{r}}t}, \tag{4.3}$$

where $\omega_i = 2\pi f_i$ is the angular frequency and E_{0i} the electric field amplitude of the i^{th} beam. Assuming, for simplicity, that the waves have the same complex amplitude, such that $E_{0\mathrm{u}} = E_{0\mathrm{r}} = E_0$, we can write Eq. (4.3) as:

$$E(t) = E_0 \left[e^{i\omega_{\mathrm{u}}} + e^{i\omega_{\mathrm{r}}t}\right]. \tag{4.4}$$

The detected photocurrent will be

$$\boxed{i(t) \propto |E(t)|^2 = 2|E_0|^2 \left(1 + \cos[(\omega_{\mathrm{u}} - \omega_{\mathrm{r}})t]\right).} \tag{4.5}$$

It should be clear that the detected signal will consist of a constant background ($|E_0|^2$) that is modulated with a frequency corresponding to the *difference* of the two optical frequencies. This frequency can be detected

using precise electronic RF techniques, provided that the frequency difference $\Delta f = |f_{\mathrm{u}} - f_{\mathrm{r}}|$ is smaller than the electronic bandwidth of the photodetector (e.g. 100 GHz). **As a consequence, knowing one of the optical frequencies precisely allows the unknown optical frequency to be determined through measuring the beat frequency (or beat note) Δf: $f_{\mathrm{u}} = f_{\mathrm{r}} \pm \Delta f$!** It should be emphasized that this type of measurement technique is known as *optical heterodyne detection*. Similar heterodyne detections are also used in the RF domain.

Figure 10 shows an example beat signal. Here, Fig. 10(a) shows the photocurrent measured for the superposition of two optical waves whose frequency difference of $\Delta f = 10$ GHz. A beat whose period $\tau_{\mathrm{per}} = \Delta f^{-1} = 100$ ps is clearly observed. The practical way of measuring the beat frequency is to direct the photodetector signal to a radio-frequency spectrum analyzer. An RF spectrum corresponds to the Fourier transform of the time-averaged electric field squared. Thus a periodic beat signal can be detected as a spike in the spectrum. The RF spectrum of the beat signal in Fig. 10(a) is plotted in 10(b), and we can identify an isolated peak at the 10 GHz beat frequency.

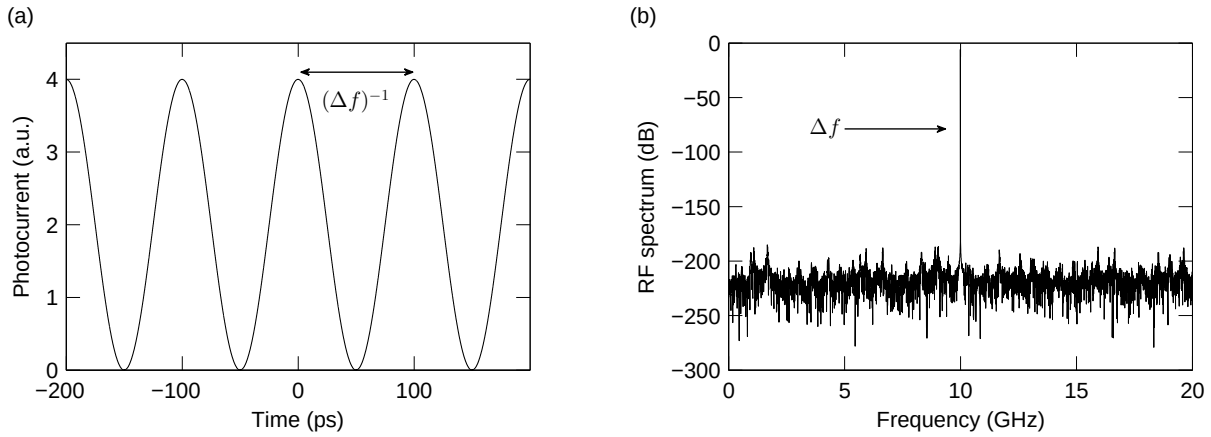

Figure 10: (a) Photocurrent corresponding to the superposition of two monochromatic EM waves with identical amplitudes but different frequencies: $i(t) = |E_1 + E_2|^2$, where $E_m = E_0 \exp(i\omega_m t)$. The waves' frequency difference $\omega_2 - \omega_1 = 2\pi \times 10$ GHz. (b) Corresponding RF spectrum.

4.3 Problem: where to get a suitable reference frequency

To start measuring unknown optical frequencies and build optical atomic clocks we can use heterodyne detection. To use heterodyne detection, however, we first need to know an optical reference frequency extremely well. Moreover, if we know a single optical reference frequency we can only measure frequencies that are translated less than 100 GHz from the reference frequency (otherwise the detector bandwidth will be unable to handle the beat note), so we would rather know a few of them.

Before optical frequency combs, the only way to derive an optical reference frequency known with a precision of some parts in 10^{14} was to start from a Cs atomic clock and multiply the frequencies through the whole electromagnetic spectrum via harmonic chains. In such chains the precisely known oscillator frequency is multiplied in steps using a wide variety of different technologies: solid state and electron tube microwave sources up to 500 GHz and lasers for higher frequencies.

Because the frequency interval from microwave Cs standards to the optical regime is enormous, more than

10 steps (and thus different laser/oscillator technologies) were required in the harmonic chain [Fig. 11 illustrates a harmonic chain used in the Physicalisch-Technische Bundesanstalt (PTB)]. Because of this, the chains could easily fill several large laboratories, were highly complex to operate, and consisted of costly devices. And of course, one chain could be used to measure only a single optical frequency (plus or minus few tens of GHz).

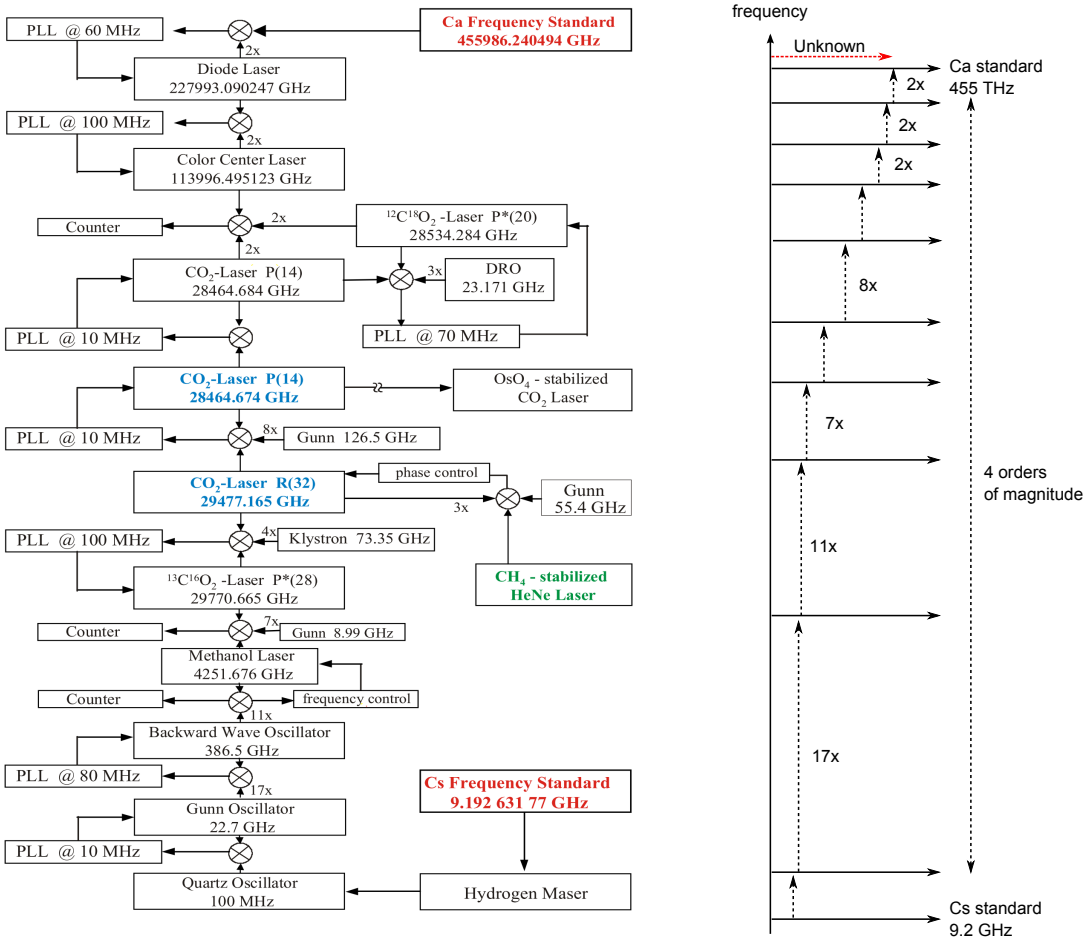

Figure 11: Schematic of the harmonic frequency chain used in the PTB. Adapted from [J. Ye and S. T. Cundiff, "Femtosecond optical frequency comb: principle, operation, and applications, " Springer, 2004.]

5 Optical frequency combs

As described above, harmonic chains can be used for absolute optical frequency measurements, but they are not very practical. A much better solution is to use an optical frequency comb: a light source whose spectrum consist of sharp, equally spaced lines. A mode-locked laser turns out to be just the source needed.

5.1 Mode-locked lasers as rulers of frequency

As discussed in Section 3.2, a mode-locked laser emits a train of ultrashort pulses separated by the cavity round trip time t_{R}. On the other hand, we also described how this pulse train arises as the coherent superposition of numerous longitudinal modes. Specifically, a mode-locked pulse train can be understood as a superposition of electromagnetic waves with different frequencies. Because the frequency separation of adjacent longitudinal modes is constant (i.e., the cavity FSR or the repetition rate f_{rep}), the *spectrum* of a mode-locked laser is indeed a frequency comb: a sequence of sharp, equally-spaced lines. This is illustrated in Fig. 12.

Because the longitudinal modes are spaced by the same constant FSR, one is led to conclude that their

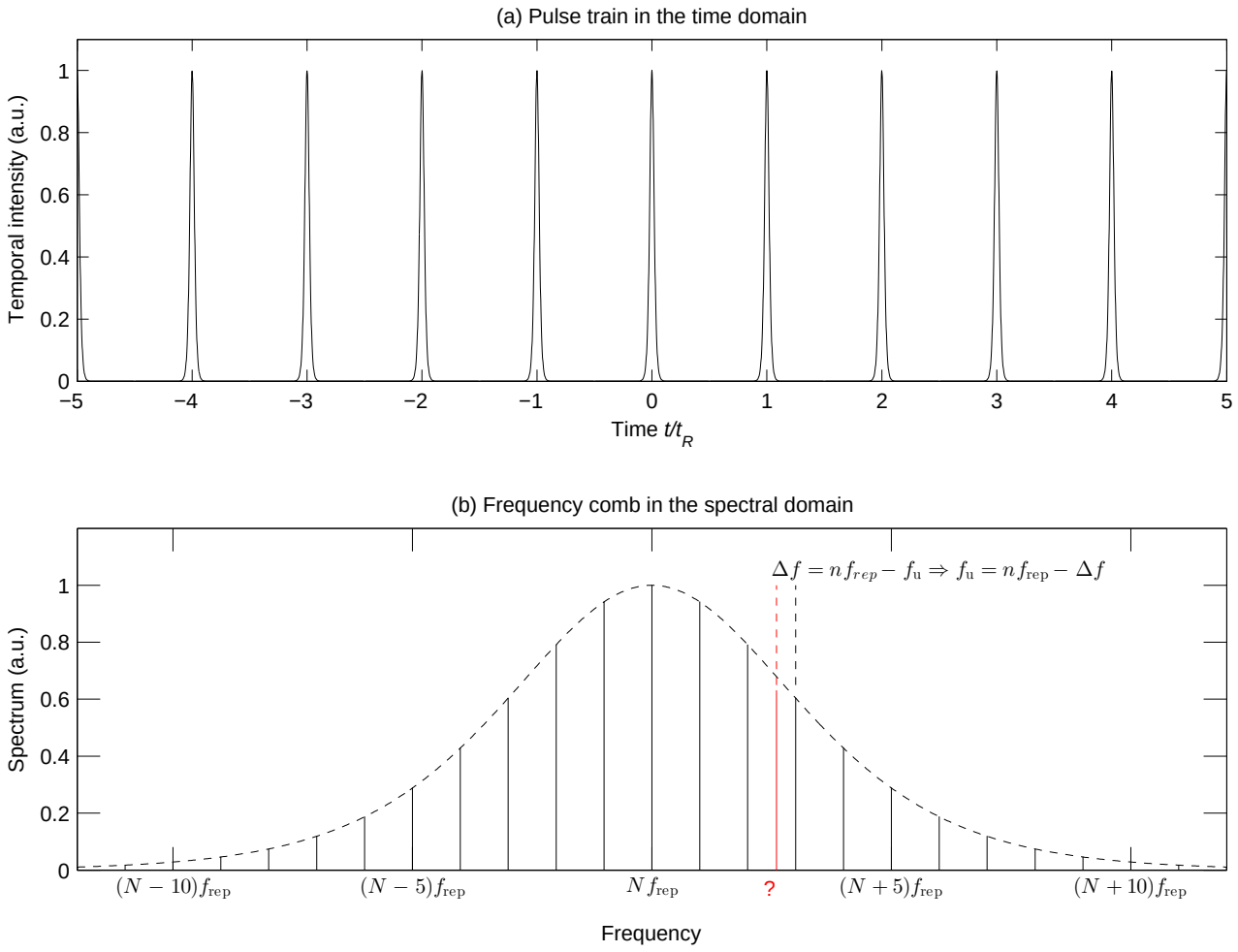

Figure 12: Schematic illustration of the spectrum of a mode-locked laser and its use for frequency metrology. (a) An infinite train of pulses regularly spaced in time by $t_{\mathrm{R}} = f_{\mathrm{rep}}^{-1}$. (b) Corresponding spectrum consisting of sharp lines spaced by f_{rep}. If the positions of the frequency comb lines are precisely known, they can be used as reference frequencies in precision heterodyne measurements.

absolute frequencies are given by

$$\boxed{f_n = n f_{\rm rep},} \tag{5.1}$$

where $f_{\rm rep}$ is the laser's repetition rate and n is an integer. Significantly, $f_{\rm rep}$ can be measured precisely simply by shining the mode-locked pulse train on a photodetector. Indeed, the repetition rate $f_{\rm rep}$ typically ranges from 10s of MHz to a few GHz for mode-locked lasers. Accordingly, the pulse train can be readily resolved on a photodetector, allowing for precise measurements of the repetition rate. But on the other hand, if $f_{\rm rep}$ is known precisely, then we actually know all the "frequency comb lines" f_n, as n is just an integer! The implications are concrete: **the frequency comb spectrum of mode-locked lasers can be used in heterodyne detection as the precisely known reference frequencies! What adds to the fun is the fact that there is generally a huge number of comb lines! Figure 12(b) illustrates the principle.**

5.2 Carrier envelope offset

Unfortunately, the scheme above does not work quite as advertised. The reason is that, while the spectral modes of a mode-locked laser are each separated by $f_{\rm rep}$ from one another, the comb is generally offset from zero frequency. This means that the mode frequencies are not given by Eq. (5.1) but rather by:

$$\boxed{f_n = n f_{\rm rep} + f_{\rm CEO},} \tag{5.2}$$

where $f_{\rm CEO}$ is known as the carrier-envelope offset frequency. This issue is illustrated in Fig. 13 which should be contrasted with Fig. 12. Although $f_{\rm CEO}$ lies within the RF regime (as a matter of fact, $f_{\rm CEO} < f_{\rm rep}$), measuring its value was beyond the capabilities of researchers until recently. **Without knowledge of $f_{\rm CEO}$ the frequencies are not absolutely known, and therefore cannot be used in heterodyne detection for precision metrology.**

The carrier-envelope offset frequency arises because the phase of the pulse is changing every round trip. This means that, as shown in Fig. 14, the phase of the carrier wave at the peak of the pulse envelope is changing every round trip: the carrier slips underneath the envelope from roundtrip to roundtrip. Mathematically, we can write the complex electric field corresponding to the pulse train as

$$E(t) = \sum_{n=-\infty}^{\infty} A(t - n t_{\rm R}) e^{i n \phi_{\rm CEO} + i \omega_0 t}, \tag{5.3}$$

where $A(t)$ is the profile of the slowly-varying envelope, ω_0 is the carrier frequency, and $\phi_{\rm CEO} = 2\pi f_{\rm CEO} t_{\rm R}$ is known as the carrier-envelope offset phase. The carrier envelope frequency should be understood as the frequency at which the phase repeats. Indeed, if the phase slips by $\phi_{\rm CEO}$ per roundtrip, it will take $N = 2\pi/\phi_{\rm CEO}$ round trips to accumulate a full 2π phase shift, and hence return to the initial value. The corresponding time is $\tau_{\rm CEO} = N t_{\rm R}$, yielding the frequency $f_{\rm CEO} = \tau_{\rm CEO}^{-1} = \phi_{\rm CEO}/(2\pi t_{\rm R})$.

The reason that mode-locked lasers generally come with a nonzero carrier-envelope offset frequency is dispersion inside the laser cavity. Specifically, the refractive indices of various components in the cavity depend on wavelength. As a consequence, the carrier wave and the pulse envelope propagate at different velocities. Indeed, the carrier wave propagates at the phase velocity

$$v_p = \frac{c}{n} \tag{5.4}$$

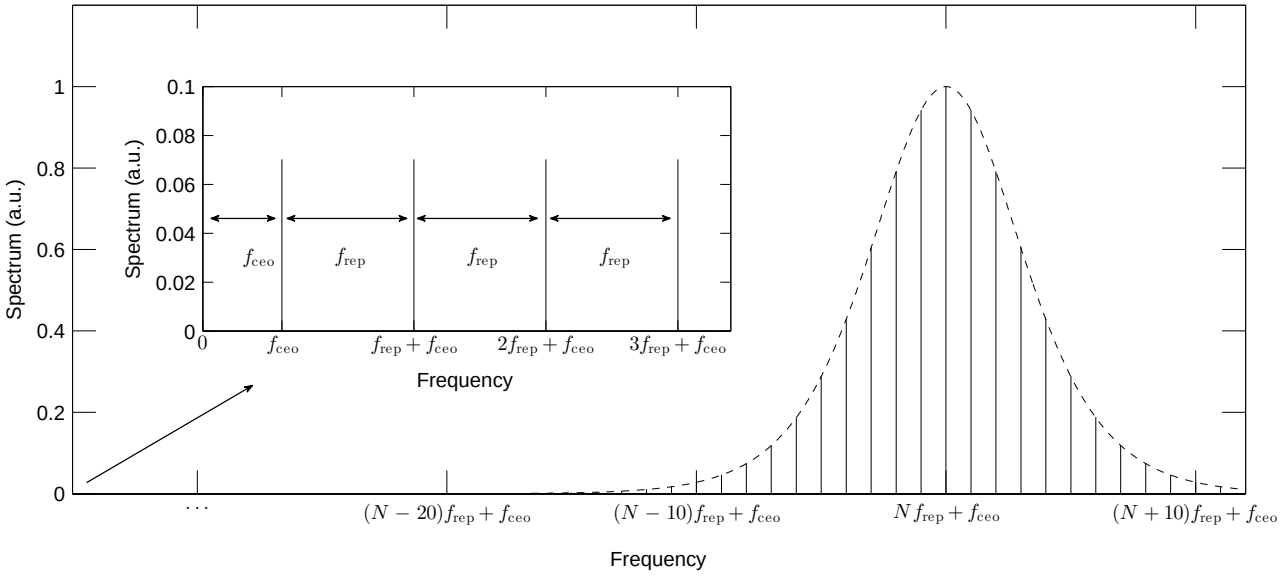

Figure 13: Spectrum of a mode-locked laser with non-zero carrier-envelope offset frequency $f_{\rm CEO}$. Although the frequency comb lines are spaced by $f_{\rm rep}$, they do not start from zero. Instead, the first comb line would be $f_{\rm CEO}$. Of course, since $f_{\rm CEO}$ is 6 orders of magnitude away from the comb's centre frequency, there is no light energy at that frequency, preventing its measurement.

whilst the envelope propagates at the group velocity

$$v_g = \frac{c}{n + ndn/d\omega}. \tag{5.5}$$

Because of dispersion, we have $dn/d\omega \neq 0$, and therefore $v_p \neq v_g$. Accordingly, it takes different times for the carrier and the envelope to complete a single roundtrip, resulting in a roundtrip-to-roundtrip phase slip.

5.3 Referencing the comb

To use the frequency comb spectrum of mode-locked lasers as reference frequencies in precision heterodyne detection, both $f_{\rm rep}$ and $f_{\rm CEO}$ must be known precisely. The repetition frequency $f_{\rm rep}$ is easy to measure by simply shining the pulse train on a photodetector. To fully reference the comb, also $f_{\rm CEO}$ must be obtained. This, however, is much more difficult owing to the fact that $f_{\rm CEO}$ involves the dynamics of the carrier wave. Indeed, considering the photocurrent $i(t) = |E(t)|^2$ generated by a mode-locked pulse train described by Eq. (5.3), we find that all traces of $f_{\rm CEO}$ disappear: only the envelope can be detected.

One way of determining the carrier-envelope offset frequency is to use a harmonic frequency chain so as to obtain an absolute reference frequency $f_{\rm r}$ within the comb bandwidth. The beat frequency of an arbitrary comb mode and the frequency chain reference is then:

$$\Delta f = |f_n - f_{\rm r}| = |nf_{\rm rep} + f_{\rm CEO} - f_{\rm r}|. \tag{5.6}$$

Because $f_{\rm r}$ is known precisely, and Δf and $f_{\rm rep}$ can easily be measured precisely, $f_{\rm CEO}$ can be deduced. Although this technique still exhibits some of the practical issues of harmonic chains, it greatly extends its

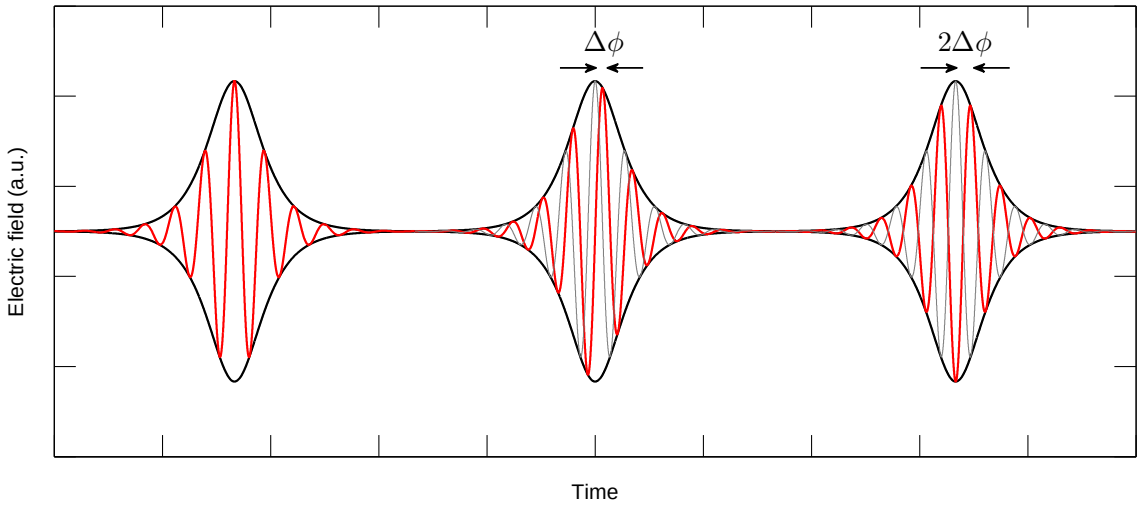

Figure 14: Schematic illustration of carrier-envelope phase slip over three consecutive pulses

application range. Indeed, referencing a single mode yields precise knowledge of all the comb lines ($f_n = nf_{\mathrm{rep}} + f_{\mathrm{CEO}}$) which allows for precision frequency measurements of optical frequencies within the whole bandwidth of the mode-locked spectrum (tens of THz). This should be contrasted with the application of a harmonic chain alone, which essentially allows for the measurement of a single frequency only (or frequencies offset by less than 100 GHz from the chain reference). The technique of referencing the mode-locked comb externally to perform frequency measurements was first used in 1999 to cover a frequency gap of 90 THz [see Udem *et al.*, Phys. Rev. Lett. **82,** 3568-3571 (1999)].

A frequency comb can be referenced even without a harmonic chain which is naturally the preferred route because harmonic chains cost millions and take a few laboratories of space. In particular, under suitable conditions the frequency comb can be **self-referenced** by performing a beat note measurement on two well-chosen frequencies within the comb.

6 Nonlinear optics to the rescue

Before describing how optical frequency combs can be self-referenced, we must discuss a branch of physics known as nonlinear optics. In most everyday life situations, the light that we encounter is weak, i.e., the electromagnetic waves possess small amplitudes. When this is the case, matter responds linearly to light.

When light is shined on an object, the oscillating electric field of the light wave will make electrons in the matter oscillate. (This is simply because the electric field exerts a force $F_e = -eE(t)$ on the electrons.) When the electric field amplitude is small, the electrons oscillate exactly at the same frequency as the electric field, say ω_0. This gives rise to a bunch of oscillating electric dipoles, which can be described by a material polarization

$$P(t) = \chi^{(1)} E(t) = \chi^{(1)} E_0 e^{i\omega_0 t}, \tag{6.1}$$

where $\chi^{(1)}$ is known as the linear electric susceptibility. Using this polarization in Maxwell's equations, we can

derive all the usual optical phenomena that we encounter in everyday lives: reflection, refraction, dispersion, birefringence, lenses, diffraction, interference, you name it. (The refractive index $n = \sqrt{1+\chi^{(1)}}$.) Because the polarization is *linearly* dependent on the electric field, we say that we are in the regime of *linear* optics.

If the electric field amplitude becomes very large, the linear relationship between the polarization and the electric field breaks. Such large electric fields can be readily obtained from lasers. Indeed, when strong laser light is incident on an object, the associated electric field will make electrons in the material oscillate such that their their motion will contain contributions from many different frequencies. The dominant contribution will come from the fundamental frequency of the light wave, ω_0, but we also find contributions from its harmonics (e.g. $2\omega_0$, $3\omega_0$,...). In this regime, the material polarization becomes

$$P(t) = \chi^{(1)}E(t) + \chi^{(2)}E^2(t) + \chi^{(3)}E^3(t) + \cdots , \tag{6.2}$$

where $\chi^{(2)}$ and $\chi^{(3)}$ are second- and third-order electric susceptibilities, respectively. We see that the polarization depends *nonlinearly* on the electric field; when the higher-order terms are significant, we say that we are in the regime of *nonlinear* optics.

An electron oscillating with a frequency ω will generate electromagnetic waves at that same frequency ω. But above, we described how a strong laser light with frequency ω_0 can make electrons oscillate with a frequency $2\omega_0$. Does this mean that, through nonlinear optics, we can generate EM waves with new frequencies? Indeed it does.

Nonlinear optics allows for the generation of new colours! In particular, through nonlinear optical processes, strong laser light at frequency ω_0 can be (partially) converted to other frequencies.

Today nonlinear optics is a very big area of research. This is because it can be used for the generation of laser light at wavelengths where no active media with suitable laser transitions exist. In 1982, the Nobel prize in physics was awarded to Nicolaas Bloembergen for his pioneering contributions to nonlinear optics.

6.1 Second-harmonic generation

Second-harmonic generation (SHG) is a nonlinear optical process that allows for the frequency-doubling of an incident laser beam. In this process, laser light with frequency ω_0 is shined on a nonlinear optical crystal, and a new laser light beam with frequency $2\omega_0$ is generated (see Fig. 15). SHG was the first nonlinear process that was discovered (in 1961), immediately following the invention of the laser. Today, SHG is widely used in many applications. Perhaps the most famous one is the green laser point.

Example

The laser light emerging from green laser pointers starts at a wavelength of 808 nm, being generated from an infrared AlGaAs laser diode. This laser light is used to optically pump a Nd:YAG laser that then emits laser light at 1064 nm. Finally, this laser light is frequency-doubled using SHG so as to obtain a wavelength of $532\ \mathrm{nm} = 1064\ \mathrm{nm}/2$. When buying green laser pointers, you want to be sure that residual infrared light at 1064 nm is blocked with a spectral filter. Otherwise you may get 10s of mW of infrared laser light out from an innocent 1 mW green laser pointer.

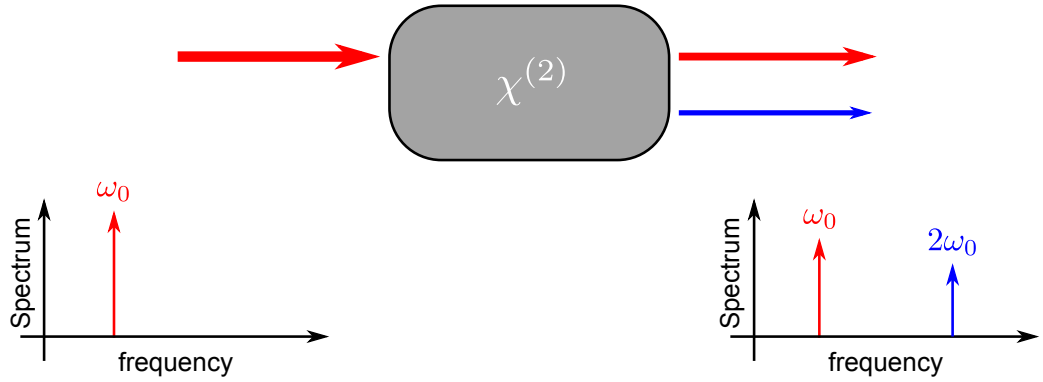

Figure 15: Schematic illustration of second-harmonic generation. An optical wave with frequency ω_0 is launched into a $\chi^{(2)}$ nonlinear crystal, resulting in the generation of a new beam at the second-harmonic frequency $2\omega_0$.

6.2 Self-referencing: f-2f interferometry

Second-harmonic generation turns out to be very useful for self-referencing optical frequency combs. Consider two specific frequencies, one at the high- and one at the low-frequency side of the spectrum, $f_n = nf_{\rm rep} + f_{\rm CEO}$ and $f_{2n} = 2nf_{\rm rep} + f_{\rm CEO}$, respectively. By doubling the low-frequency component in a second-order nonlinear crystal using second-harmonic generation, we obtain the frequency $2f_n = 2nf_{\rm rep} + 2f_{\rm CEO}$. Beating the second-harmonic frequency $2f_n$ with the high-frequency component f_{2n}, we measure the note

$$\begin{aligned} \Delta f &= |2f_n - f_{2n}| && (6.3)\\ &= |2nf_{\rm rep} + 2f_{\rm CEO} - 2nf_{\rm rep} - f_{\rm CEO}| && (6.4)\\ &= f_{\rm CEO}. && (6.5) \end{aligned}$$

The beat note can be seen to correspond to $f_{\rm CEO}$, which can now be measured at high precision using established RF techniques.

The technique described above is known as interferometric $f - 2f$ self-referencing and its principle is schematically depicted in Fig. 16. Measuring $f_{\rm CEO}$ as a beat note not only allows for the full referencing of the comb but also allows for $f_{\rm CEO}$ to be arbitrarily controlled. The latter is achieved by monitoring the beat note while changing the length of the cavity using a piezoelectric controller. Changing the cavity length L allows the carrier-envelope phase offset to be controlled.

6.3 Difficulty in self-referencing

Self-referencing a mode-locked frequency comb allows for simple measurement of absolute optical frequencies. Indeed, as knowledge of $f_{\rm rep}$ and $f_{\rm CEO}$ allows each comb line to be precisely identified, $f_n = nf_{\rm rep} + f_{\rm CEO}$, any one of the lines can be used as an absolute reference frequency. It is precisely the ideas and techniques outlined above that resulted in the Nobel prize of physics in 2005: (i) the fact that the spectral lines of a mode-locked comb can be used as absolute reference frequencies in heterodyne detection and (ii) the fact that such a comb can be self-referenced.

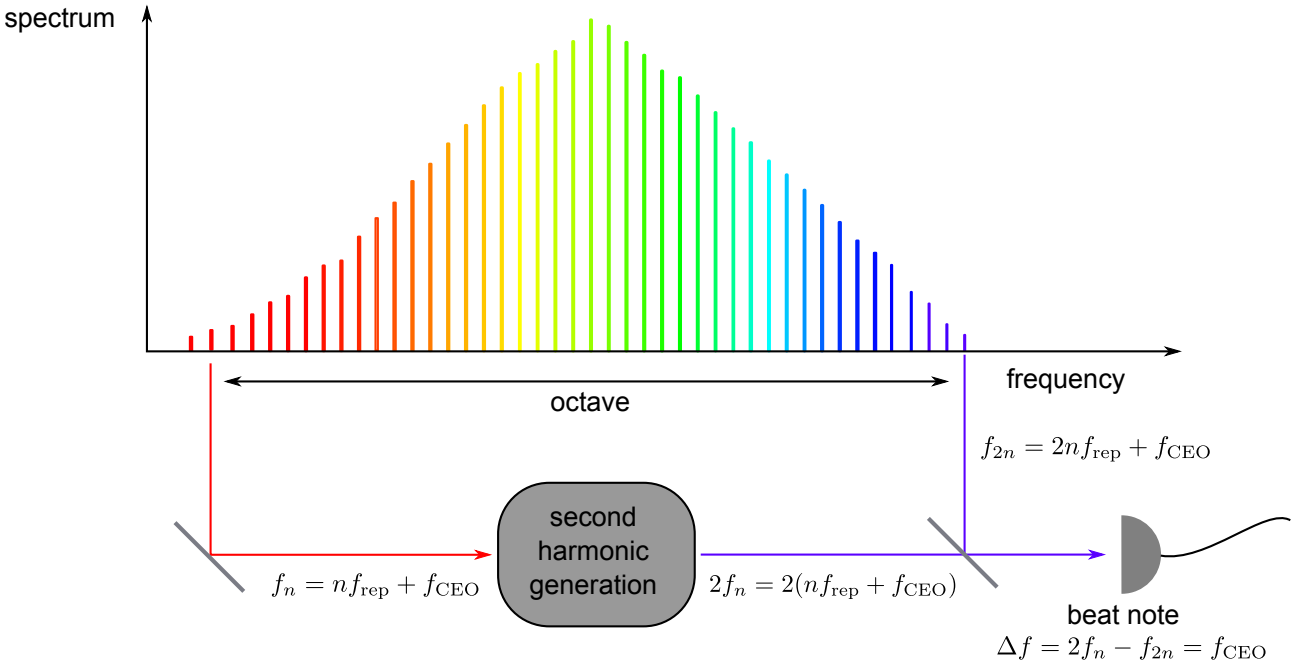

Figure 16: Schematic illustration of interferometric $f - 2f$ self-referencing.

The $f - 2f$ self-referencing of a mode-locked laser was first demonstrated in 2000, while the first mode-locked laser was demonstrated in 1964. The difficulty lies in the fact that the two frequencies needed for self-referencing must be separated by almost an optical octave, i.e. $f_{2n} \sim 2f_n$. This means that the emission bandwidth of the laser must satisfy $f_{2n} - f_n > f_0$, where f_0 is the center frequency, of the order of 200 THz. The bandwidth of typical mode-locked lasers is significantly smaller. For example, commercial Ti:Sapphire lasers typically emit over a bandwidth of about $\Delta f \approx 15$ THz. Thus the obstacle in using mode-locked lasers for frequency metrology was to obtain a spectrum sufficiently broad to allow for self-referencing through $f-2f$ interferometry. This obstacle was not overcome until 2000.

7 Femtosecond supercontinuum generation

In order to obtain a spectrum spanning more than an optical octave, the laser output of an ultrashort oscillator must be externally broadened. This is possible by exploiting extreme nonlinear effects in optical fibers.

Conventional optical fibres consist of a core whose refractive index is higher than the surrounding cladding; light is confined in the fibre through total internal reflection. Because the core size is very small (e.g. about 10 μm in conventional fibres), fibres can confine light in a very small area. This gives rise to large electric field amplitudes. Furthermore, optical fibres can be hundreds of metres long, allowing light-matter interactions to accumulate over large distances. Thus, optical fibres at least superficially appear very suitable for the creation of new frequencies through optical nonlinearities: large electric field amplitudes and large interaction lengths.

Unfortunately, the linear and nonlinear properties of conventional optical fibres are far from ideal for nonlinear optics. Briefly, spectral broadening in optical fibres is governed (to first order) by the interplay of two material parameters:

Key parameters of nonlinear fibre optics

1. **Nonlinearity coefficient γ:** describes the strength of the nonlinear interactions.
2. **Group-velocity dispersion (GVD) coefficient β_2:** describes the temporal broadening of a short pulse propagating in the fibre.

These parameters are tied to the fibre at hand, and as such, they represent *material* parameters. The actual nonlinearities that occur also of course depend on the electric field amplitude – or equivalently – on the peak power of the pulse launched into the fibre. Larger peak power imply larger electric field amplitudes, hence stronger nonlinear effects. Mathematically, propagation of the slowly-varying pulse envelope $A(t, z)$ along the fibre is described (to first order) by the following partial differential equation:

$$\frac{\partial A}{\partial z} = -i\frac{\beta_2}{2}\frac{\partial^2 A}{\partial t^2} + i\gamma|A|^2 A. \tag{7.1}$$

This equation has the form of the Schrödinger's equation with a nonlinear potential $V = |A|^2$, and is indeed referred to as the nonlinear Schrödinger equation.

To optimise spectral broadening, the coefficients γ and β_2 should satisfy certain conditions. First γ should be as large as possible so as to enhance the nonlinear interactions. On the other hand, β_2 should be as small as possible to prevent significant pulse broadening and hence allow large peak power to be maintained for large distances. Furthermore, for reasons that we shall not describe in detail, the sign of β_2 should be negative, i.e., $\beta_2 < 0$. When this is the case, we say that the group-velocity dispersion is **anomalous**.

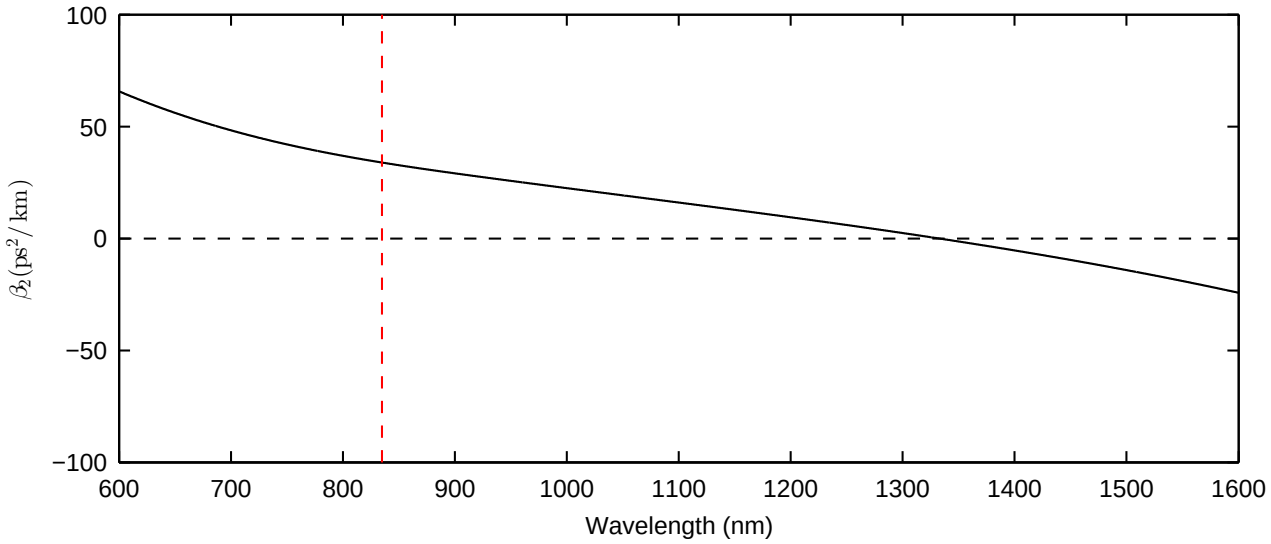

Figure 17: Group velocity dispersion β_2 as a function of wavelength for a standard telecommunication fibre. Dashed horizontal line indicates the zero-dispersion point ($\beta_2 = 0$), while dashed vertical line indicates the centre wavelength of the Ti:Sapphire laser.

Unfortunately, the γ and β_2 coefficients of conventional optical fibres are not ideal for spectral broadening. First, conventional fibres have a very small nonlinearity coefficient $\gamma \approx 1\ (\mathrm{Wkm})^{-1}$. Second, the GVD coefficient β_2 is large and positive at wavelengths where mode-locked lasers operate. Indeed, Fig. 17 shows a plot of β_2 as a function of wavelength for a standard telecommunication fibre (SMF-28). Also highlighted is the 835 nm centre wavelength of Ti:Sapphire lasers – which until recently were the only mode-locked laser with sufficient stability needed for frequency metrology. As can be seen, the GVD coefficient of SMF-28 is very large and positive at that wavelength, preventing efficient spectral broadening. This is illustrated in Fig. 18, where we show numerically simulated spectral and temporal evolutions of an ultra-short pulse propagating through 4 m of SMF-28. Because of the large GVD, the pulse undergoes rapid temporal broadening [Fig. 18(b)], resulting in equally rapid reduction in peak power. As the peak power reduces, the nonlinear interactions correspondingly cease, and we see negligible spectral broadening [Fig. 18(a)].

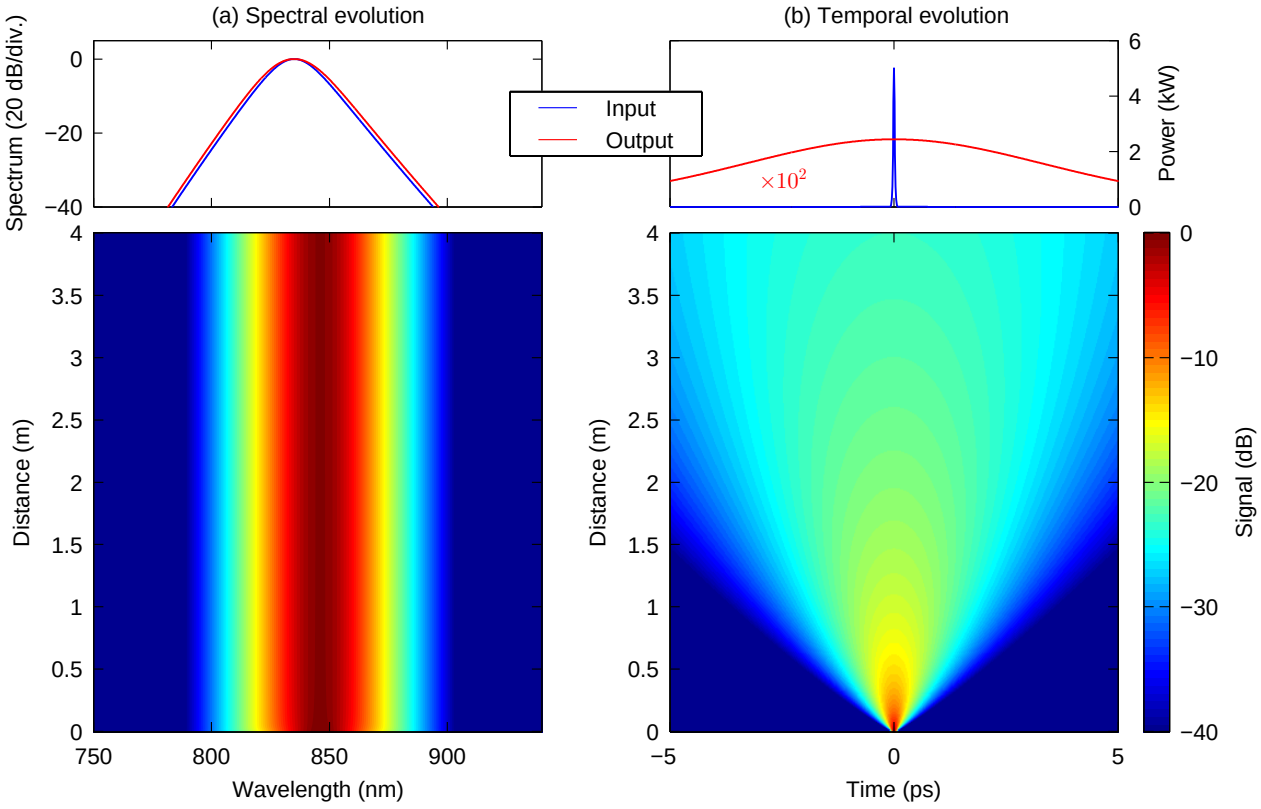

Figure 18: Numerical simulation results, showing the (a) spectral and (b) temporal evolution of a 50 fs pulse with 5 kW peak power propagating through a 4-m-long segment of standard optical fibre. The insets above show spectral and temporal profiles at the fibre input and output, respectively. The output temporal profile is magnified one-hundred-fold to be visible.

7.1 Photonic crystal fibers

Although sufficient spectral broadening in single-mode fibers had been demonstrated already in the 1970s, these experiments were conducted using long pulses from non-mode-locked lasers. Reaching similar spectral expansion from a mode-locked Ti:Sapphire oscillator was prevented by the lack of fibers with suitable nonlinearity and dispersion characteristics, and was not achieved until year 2000.

The technological breakthrough that enabled extreme spectral broadening of mode-locked Ti:Sapphire oscillators was the development of a new kind of optical fibre, known as the **photonic crystal fibre**. In ordinary step-index fibers a core of high refractive index is surrounded by a cladding of slightly lower refractive index with light guidance occurring through total internal reflection [see Fig. 19(a)]. To the contrary, in a PCF, a regular array of air holes run through the whole fiber, resulting in a fiber cross-section as that shown in Fig. 19(b). Although light is still guided through total internal reflection owing to a core-defect corresponding to a missing air-hole, the fibre's dispersion characteristics can be dramatically tailored by varying the size and separation of the air holes. In particular, it is possible to push the zero-dispersion wavelength (wavelength at which $\beta_2 = 0$) to wavelengths significantly shorter than what is possible with single-mode fibers. Example profiles of two different PCFs are shown in Fig. 20, compared with the profile of an ordinary single-mode fiber. One of the PCFs can be seen to have the zero-dispersion wavelength around 800 nm, precisely in the vicinity of the Ti:Sapphire emission band. In addition to the flexible dispersion profile, the optical mode is much more tightly bound in PCFs than in ordinary step-index fibers owing to which the nonlinearity coefficient of PCFs can be up to two orders of magnitude larger than for conventional fibers.

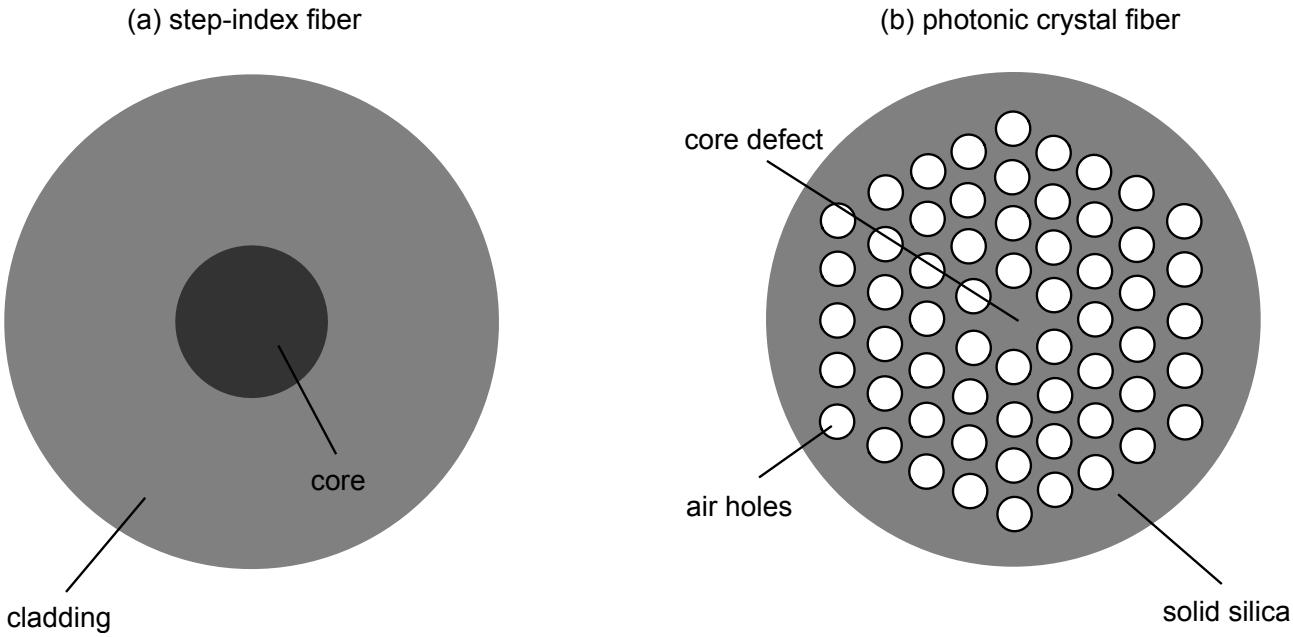

Figure 19: Schematic illustrations of the cross-sections of a conventional step-index fiber (a) and a solid-core photonic crystal fiber (b).

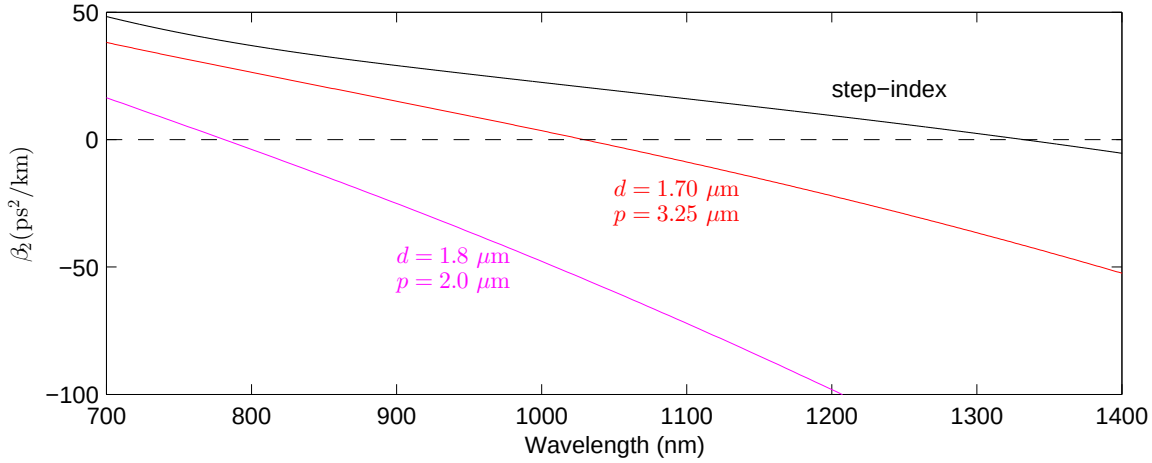

Figure 20: Group-velocity dispersions as a function of wavelength for a conventional step-index fiber (black) and two different photonic crystal fibers (red and magenta). The design parameters of the PCFs are: 1.8 μm hole diameter and 2.0 μm pitch (magenta) and 1.70 μm hole diameter and 3.25 μm pitch (red). Dashed horizontal line indicates zero-dispersion.

7.2 Supercontinuum generation

The first PCFs emerged in 1999. Already in 2000, Jinendra Ranka and co-workers at the Bell Labs performed a landmark experiment, where they launched ultrashort (100 fs) pulses from a Ti:Sapphire laser centered at 800 nm through a 75 cm long piece of PCF [J. K. Ranka *et al.*, Opt. Lett. **25**, 25-27 (2000)]. Remarkably, the group witnessed the transformation of the narrowband (10 nm) input spectrum into a broad spectral continuum (neatly named, supercontinuum) ranging from 400 nm to 1600 nm — more than an optical octave. Figure 21 shows results from numerical simulations that illustrate the spectral broadening inside the PCF.

It was quickly realised that supercontinuum generation in a PCF was the missing link needed to make optical frequency combs work. Indeed, the first optical frequency comb self-referenced using the $f - 2f$ method was demonstrated in 2000, using precisely the Ti:Sapphire -based supercontinuum technology demonstrated by Ranka *et al.* [D. J. Jones *et al.*, Science **288**, 635-639 (2000)]. With this result, it immediately became possible to use frequency combs corresponding to mode-locked pulse trains to precisely measure unknown optical frequencies. Within a very short time period, this ability triggered numerous breakthroughs across the natural sciences, ranging from improved measurements of physical constants to the realisation of all-optical atomic clocks. In 2005, the inventors of the frequency comb technique – John Hall and Theodore Hänsch – were awarded half the Nobel prize in physics. Today, optical frequency combs remain a very active area of research.

In addition to enabling self-referencing of optical frequency combs, fibre supercontinuum generation has found numerous other applications. For example, it can be used as an extremely versatile source for spectroscopy. Normally spectroscopy of different materials requires lasers at different wavelengths; however, a supercontinuum source emits all the wavelengths at once, and so the user can select any wavelength of interest using spectral filters. It is interesting to note that the supercontinuum spectra typically encompass all the visible wavelengths, which means that the emission has the appearance of white light. Yet, the supercontinuum source still maintains the high directionality and brightness attributed to laser light. Accordingly, supercontinuum sources can be understood to generate **white laser light**. This extreme example underlines how laser light is

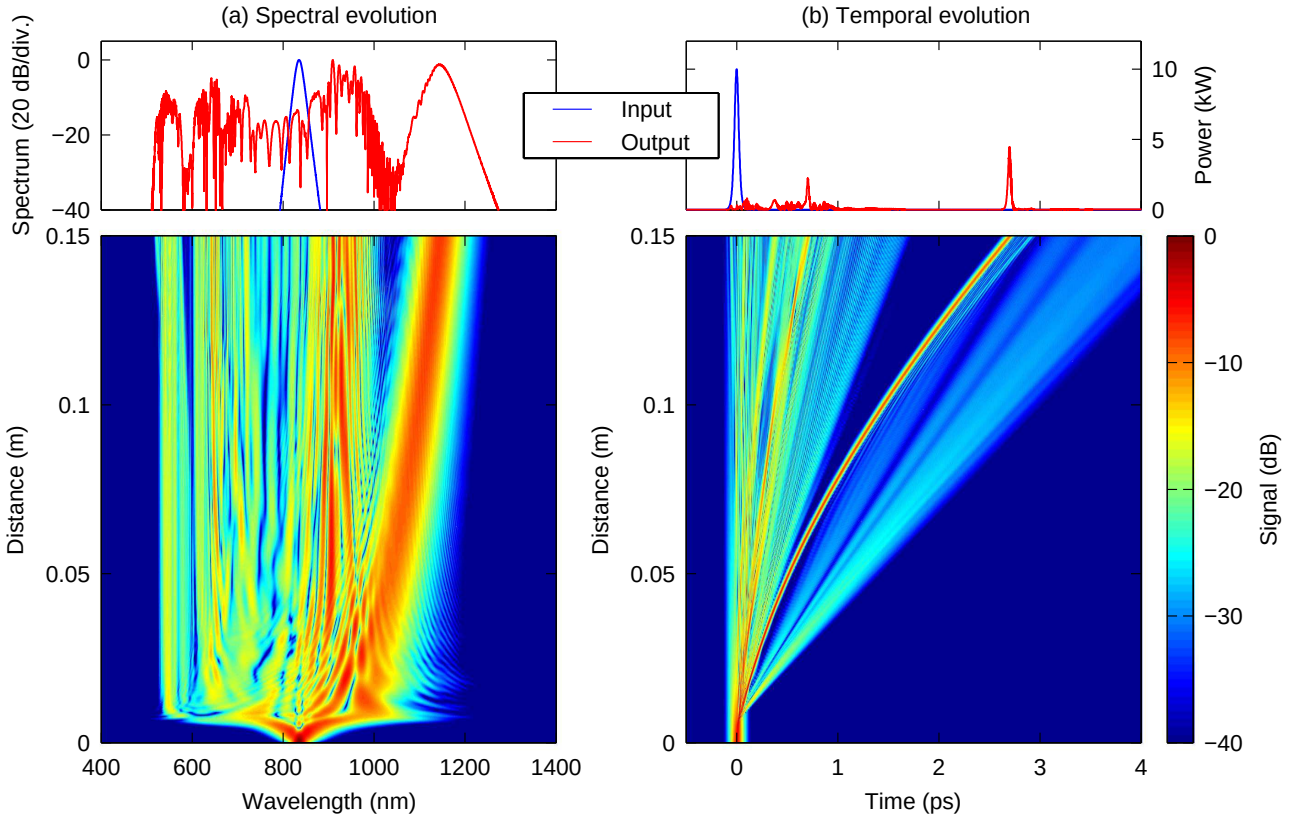

Figure 21: Spectral (a) and temporal (b) dynamics of a 50 fs, 10 kW peak power pulse propagating through 15 cm of highly nonlinear PCF. Bottom plots show the full evolution as dynamical density maps, whilst the top plots show the input and output profiles in more detail.

not *always* monochromatic, but can actually encompass all visible wavelengths (and more)!

8 Microresonator frequency combs

All commercially available frequency comb sources rely on mode-locked laser and fibre supercontinuum technologies. They have, however, certain deficiencies that make them non-ideal for particular applications. For instance, they are somewhat bulky and expensive, and can only be used to create combs whose teeth spacing is less than a few GHz. The latter restriction stems from the difficulty of designing mode-locked lasers with repetition rates larger than a few GHz, owing to the fact that repetition rate scales inversely with the length of the cavity ($f_{\mathrm{rep}} \approx c/L$). A 10 GHz repetition rate would, for example, require a cavity length of $L \approx 3$ cm, which clearly makes for a rather small laser. Given that many applications (e.g. telecommunications) would benefit from larger comb spacings, researchers have looked for alternative methods to create frequency combs.

In 2007, one such alternative was discovered [P. Del'Haye et al., Nature **450**, 1214–1217 (2007)]. Specifically, it was shown that a low-power monochromatic continuous wave (cw) laser coupled into a *microresonator* — a microscopic loop made of a dielectric material such as glass — spontaneously transformed into a fre-

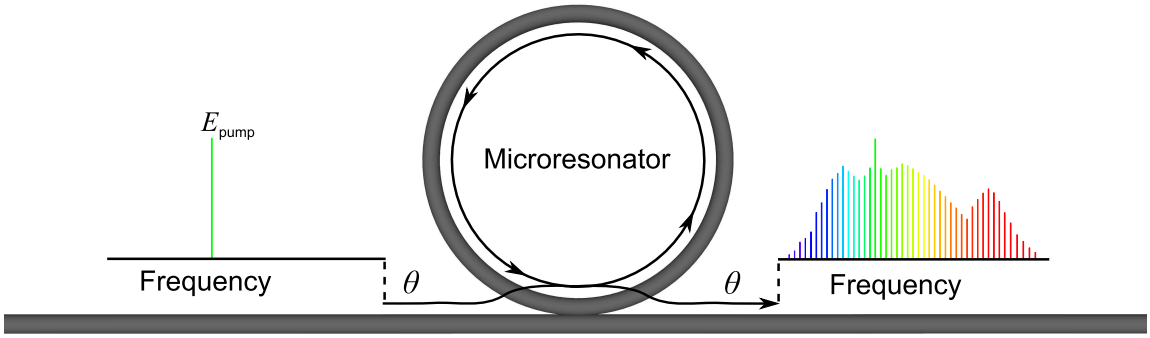

Figure 22: Schematic illustration of frequency comb generation in a microresontor. A low-power continuous wave (cw) laser beam is injected into a microscopic resonator, transforming into a broadband frequency comb due to optical nonlinearities.

quency comb [see Fig. 22]. Thanks to the microscopic cavity size, very large comb spacing up to hundreds of GHz was realised.

The ability to create frequency combs with unique characteristics using a microscopic device driven with a low-power laser attracted tremendous interest, and has rapidly grown to become one of the hottest topics in contemporary photonics.

8.1 Microresonator characteristics

Microresonators can be understood as very small loops of dielectric waveguides; like a very short piece of optical fibre looped on itself. Just like two mirrors facing each other, they correspond to optical resonators. Accordingly, they display longitudinal modes and associated resonance frequencies. Just like for a cavity made of two mirrors, the resonance frequencies are equally-spaced in frequency, and their free-spectral range FSR $= c/(nL_{\text{tot}})$, where L_{tot} is total round trip length. Because of their small dimensions, microresonators can have very large FSRs:

Example.

One way of creating a microresonator is to melt the tip of a conventional optical fibre. The melted glass ($n \approx 1.45$) forms a perfect sphere thanks to surface tension. Consider such a microsphere with a typical radius $R = 125\ \mu\text{m}$. The resonator will have a free-spectral range of

$$\text{FSR} = \frac{c}{nL_{\text{tot}}} = \frac{c}{n2\pi R} \approx 270\ \text{GHz}. \tag{8.1}$$

A key property of microresonators is that they can display extremely low losses. What this means is that, if light is launched into the resonator, it can circulate there for a long time before being dissipated through absorption or scattering. In other words, over one round trip, negligible amount of light energy is lost. Such low losses require that the resonator surface is smooth at the nanometre scale, which makes fabrication challenging. For microspheres fabricated by melting the end of a fibre tip (as in the above example), sufficient smoothness can be realised thanks to the tendency of surface tension to form perfect spheres.

Resonator losses are quantified with a parameter known as cavity finesse $\mathcal{F}$. This parameter is inversely proportional the losses per round trip, and hence large finesse corresponds to a high-quality, low-loss resonator. Formally, finesse is defined as the ratio of the cavity FSR to the full-width at half maximum of a single resonance frequency, Δf:

$$\boxed{\mathcal{F} = \frac{\text{FSR}}{\Delta f}.} \tag{8.2}$$

However, for $\mathcal{F} \gg 1$, it can be shown that the following approximation holds:

$$\boxed{\mathcal{F} \approx \frac{2\pi}{\rho},} \tag{8.3}$$

where ρ is the total loss expressed as a fraction of light energy (or power) lost over one round trip. This means that, if there is no new light injected into the resonator, then the power lost from the resonator after one round trip is

$$P_{\text{dis}} = \rho P_{\text{in}}, \tag{8.4}$$

where P_{in} is the intracavity power in the beginning of the round trip. (It should be clear that the power left after one round trip is $(1-\rho)P_{\text{in}}$.)

Example.

In a recent work [Yi et al., Optics Letters **41**, 2037 (2016)] investigated frequency comb generation in a silica wedge microresonator. In that resonator, the total loss per roundtrip was measured to be $\rho = 1.4 \times 10^{-4}$. This corresponds to a finesse of about

$$\mathcal{F} = \frac{2\pi}{\rho} \approx 45,000. \tag{8.5}$$

Let us compare these parameters to those encountered in typical mirror-based laser cavities. Considering a cavity made of two mirrors, one of which is fully reflective, while the other reflects only 95% of incident light. (Note that one mirror must be partially reflective, as otherwise no laser light can ever come out.) In this system, the total loss $\rho = 0.05$, yielding a finesse of

$$\mathcal{F} = \frac{2\pi}{\rho} \approx 125. \tag{8.6}$$

Even this value is very optimistic for actual mirror-based resonators. The moral of the story is that microresonators can have extraordinarily large finesse!

8.2 Intracavity power

Microresonators are *passive* devices: they do not contain an active medium, and hence, they are not lasers. Accordingly, to get light into the resonator, the resonator must be externally driven, i.e., laser light must be continuously injected (or coupled) into the device. This can be achieved using so-called evanescent coupling

techniques. For example, when laser light is coupled to a tapered optical fibre (with a waist diameter of the order of wavelength) some (evanescent) part of laser light will propagate outside of the taper. By bringing this taper region close to a microresonator, the evanescent field outside the taper can overlap with the evanescent wave of a cavity mode, and tunnel into the device.

As laser light is injected into a microresonator, the intracavity power level will initially increase. However, eventually the intracavity field will reach a steady-state. When the driving laser frequency coincides with a cavity resonance frequency, the steady-state intracavity power reaches its maximum value. This value can be written as[4]

$$P_{\max} = \frac{\mathcal{F}}{\pi} P_{\text{pump}}, \tag{8.7}$$

where P_{pump} is the power of the laser light injected into the resonator. Because microresonators can have very large finesse, the intracavity power can reach enormous values:

Example.

Considering the same work as above [Yi et al., Optics Letters **41**, 2037 (2016)], the researches launched 22 mW of laser power into their resonator with a finesse of about $\mathcal{F} = 45,000$. This yields an intracavity power

$$P_{\max} \approx 315 \text{ W}. \tag{8.8}$$

At approximately 5 orders of magnitude above a standard laser pointer, this represent an enormous amount of laser power. Whilst similar power levels can be used to cut and weld metals, they do not damage the microresonator because the absorption is so low (otherwise losses would be large).

8.3 Mathematics of linear cavity resonances

It is straightforward to analyse the behaviour of microresonators (or any old ring resonator) in the linear regime. Considering the scenario depicted in Fig. 22, a driving field with amplitude E_{pump} is coherently injected into the resonator every round trip with a power transmission coefficient θ. As the field propagates over round trip, it accumulates a phase shift $\phi = kz = \beta L$, where β and L are the propagation constant and circumference length of the resonator. Furthermore, as described above, some part of the intracavity power is dissipated. When the field has completed one full round trip, the driving field is again coherently superimposed on the intracavity field.

The processes outlined above can be described by the following infinite-dimensional map, which describes the evolution of the intracavity field envelope from one roundtrip to the next:

$$E_{n+1} = \sqrt{\theta} E_{\text{pump}} + \sqrt{1-\rho} E_n e^{i\phi}. \tag{8.9}$$

In steady-state, the field does not change from one round trip to the next, so we have $E_{n+1} = E_n$. This allows

[4] Here we assume the coupling to be "critical".

us to solve for the intracavity power P_{in} as a function of the round trip phase shift ϕ. We obtain:

$$P_{\text{in}}(\phi) = \frac{\theta P_{\text{pump}}}{2 - \rho - 2\sqrt{1-\rho}\cos(\phi)}. \tag{8.10}$$

It should be clear that the intracavity power is a periodic function in ϕ. The function is maximised when $\phi = 2\pi m$, with m an integer. Recalling that $\phi = \beta L = 2\pi/\lambda L$, we obtain the following resonance wavelengths

$$\lambda_m = \frac{L}{m}. \tag{8.11}$$

Indeed, these wavelengths agree precisely with Eq. (3.1). It should thus also be clear that, in frequency, the maxima of Eq. (8.12) are separated by FSR $= c/(n_{\text{eff}}L)$, where n_{eff} is effective refractive index corresponding to the propagation constant β. Finally, when the driving field is exactly on-resonance, the intracavity power levels are given by

$$P_{\text{max}} = P_{\text{in}}(2\pi m) \approx \frac{2P_{\text{pump}}}{\rho}, \tag{8.12}$$

where we assumed "critical coupling", such that $\theta = \rho/2$, as well as large finesse such that $\sqrt{1-\rho} \approx 1 - \rho/2 - \rho^2/8$. Using Eq. (8.3), we now obtain the expression presented earlier for the intracavity power [see Eq. (8.7)].

In Fig. 23 we plot the intracavity power as a function of frequency (hence, ϕ) for a resonator whose FSR = 100 GHz. Because the width of a single resonance Δf = FSR$/\mathcal{F}$ [see Eq. (8.2)], it should be clear that microresonators with very large finesse have very narrow resonances. To facilitate visualisation, in Fig. 23 we have used a low finesse of $\mathcal{F} = 50$.

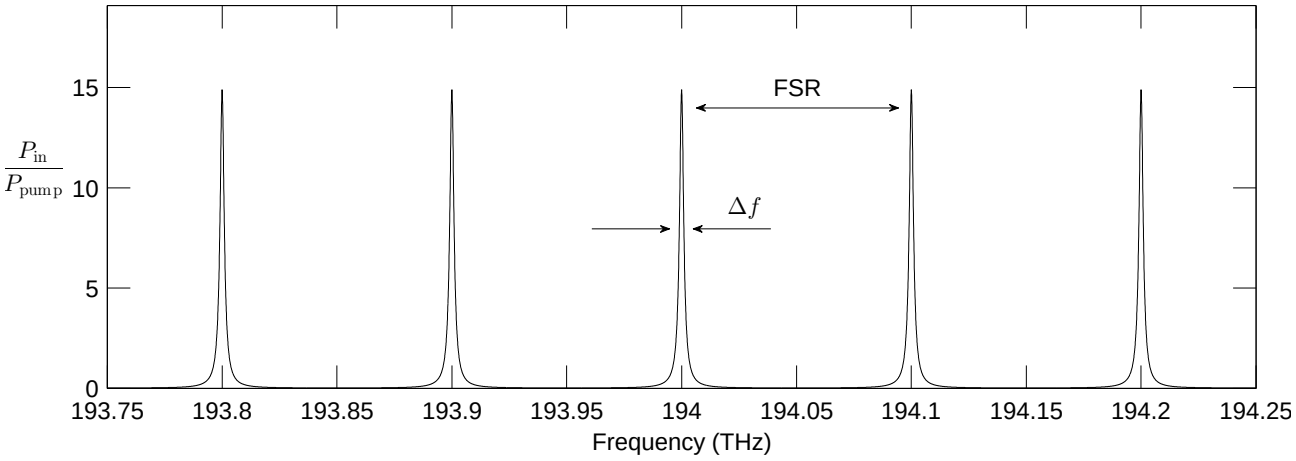

Figure 23: Examples of cavity resonances for a 100 GHz resonator with finesse $\mathcal{F} = 50$. The plot shows the ratio of intracavity power P_{in} and the driving power P_{pump} as a function of frequency.

8.4 Physics of microresonator frequency combs

Because of their small size, and the fact that the intracavity power can be so large, microresonators can show very significant optical nonlinearities even for very low pump powers (of the order of milliwattts). Through these optical nonlinearities, a low-power continuous wave laser beam injected into the resonator can transform into a broadband optical frequency comb with hundreds or even thousands of components (spaced by the cavity FSR).

The nonlinear optical process that underpins the generation of microresonator frequency combs is known as four-wave mixing. Through this process, two pump photons combine to form so-called "signal" and "idler" sidebands. Thanks to energy conservation, the sidebands are symmetrically detuned with respect to the pump:

$$2\omega_0 = (\omega_0 + \Omega) + (\omega_0 - \Omega), \tag{8.13}$$

where Ω describes the sidebands' frequency shift from the pump. The generated sidebands subsequently interact with each other and the pump wave to create a new set of sidebands. This process continues in a cascaded fashion until eventually a steady-state situation is reached. In steady-state, one finds that the intracavity (and extracavity) field corresponds to an optical frequency comb with a spacing of one cavity FSR [see Fig. 24].

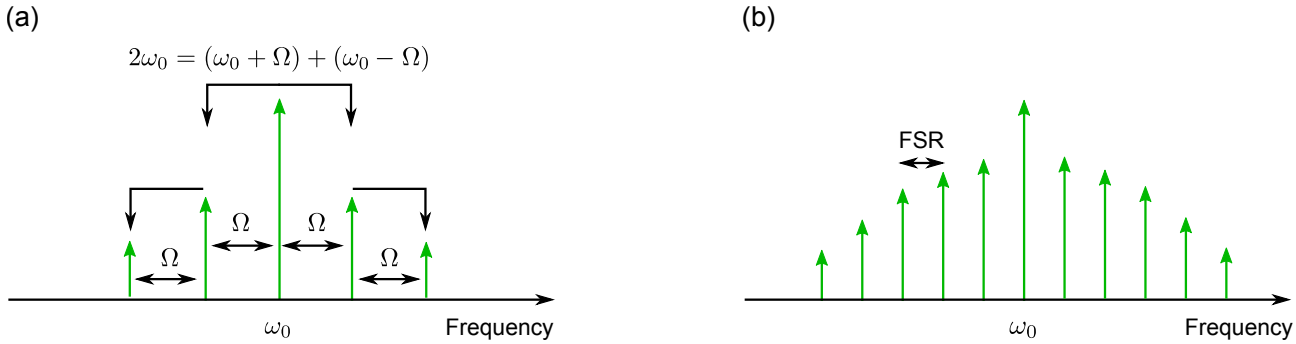

Figure 24: Schematic illustration of the nonlinear optics behind microresonator frequency combs. (a) Two pump-photons combine to create two photons whose frequencies are symmetrically detuned with respect to the pump. Further sidebands are created in a cascaded fashion as the sidebands interact with each other and the pump. (b) In steady-state, a comb with a spacing of one FSR is created.

8.5 Microresonator fabrication

The first microresonator frequency comb was demonstrated in 2007, and today the subject corresponds to one of the hottest topics in photonics. Researchers have demonstrated frequency combs in a variety of different types of resonators, including silica microtoroids, crystalline resonators made from magnesium fluoride or calcium fluoride, silica microrods, silica microspheres, and planar resonators fabricated from silicon nitride and even silicon.

Fabrication is a key challenge in microresonator research due to the need to achieve extremely large finesse. In general, different resonator materials call for different fabrication techniques. For example, crystalline resonators require mechanical cutting and/or polishing, whilst silica microrods and microspheres can be fabricated

by melting glass with a plasma arch or a CO_2 laser. Many planar resonators (e.g. silicon nitride) can be fabricated using CMOS (complementary metal oxide semiconductor) -compatible techniques, e.g. lithography. This means that they can be fabricated using existing semiconductor infrastructures, which makes them very attractive. Indeed, the dream is that eventually (microresonator) frequency comb generation can be achieved on a single integrated chip with small footprint and low power consumption. Exciting research results have recently been published that demonstrate the feasibility of this dream [D. T. Spencer et al., Nature **557**, 81 (2018)].

8.6 Applications of microresonator frequency combs

Microresonators share many of the applications of conventional mode-locked laser frequency combs. Indeed, they can be used for precision frequency metrology and for the construction of all-optical clocks. They possess however the key advantages of small footprint, power efficiency, and prospect for mass-manufacturing. Whereas mode-locked lasers are always tied to specialized research laboratories, mass-manufactured integrated microresonator devices could allow frequency combs to be used in hand-held devices and with greater flexibility. Nevertheless, it is worth emphasising that, when it comes to absolute precision, microresonators are unlikely to beat the best mode-locked laser systems due to the latters' superior stability characteristics.

Microresonator frequency combs also open up new applications that are not accessible using conventional mode-locked laser combs. Telecommunications represents a very exciting example. Indeed, today's long-haul fibre-optic communication infrastructure is based on so-called "dense wavelength division multiplexing (D-WDM)", whereby information is encoded on many individual lasers with slightly different frequencies so as to improve the amount of data that can be transmitted through a single optical fibre. The frequency-spacing in such WDM grids ranges from 12.5 GHz to 100 GHz, which is precisely in the ball-park of microresonator frequency combs. Accordingly, one could imagine replacing the hundred-or-so individual lasers used in existing systems with a single laser and a microresonator, thus improving the systems' power and cost efficiency. Very exciting research results along these lines have recently been published [P. Marin-Palomo, Nature **546**, 274 (2017)].

Another interesting application somewhat unique to microresonator frequency combs is calibration of astronomical spectrographs. For example, detection of extrasolar planets using the radial velocity methods requires the ability to precisely measure the frequencies of light emanating from distant stars. This is achieved using spectrographs, which need to be calibrated. Unfortunately, the sources used for calibration currently represent a limiting factor in the measurement precision. It has been shown that frequency combs allow the calibration precision to be improved dramatically [T. Wilken et al., Nature **485**, 611 (2012)]. Ideally, the comb source used for such calibration has a spacing of about 10 GHz. Whilst not impossible, achieving such spacing with mode-locked lasers is challenging. Microresonators, however, would appear a much more natural candidate.

Exercise problems

Question 1: On lasers.

(a) List the three key components of any laser, and **briefly** explain their role in enabling laser operation.

(b) There are three mechanisms through which light can mediate transitions between atomic energy levels. With the help of a drawing, explain what these mechanisms are and how they differ from each other.

(c) Before lasers, there were masers (microwave lasers). The first such maser was demonstrated in 1954, and it operated at a frequency $f = 24$ GHz. The first laser, on the other hand, was demonstrated in 1960 at the wavelength $\lambda = 694$ nm. Estimate the ratio N_2/N_1 between the populations of the upper and lower states of the active transition in both cases, assuming room temperature (293 K) and thermal equilibrium (such that the relative populations are governed by the Bolzmann distribution). How can the results explain the historical development of masers and lasers?

(d) The total intensity (power per unit surface area) radiated by a black body across all wavelengths is given by Stefan-Boltzmann law:

$$\frac{P}{A} = \sigma T^4, \tag{8.14}$$

where T is the temperature of the black body (in Kelvins) and the Stefan-Boltzmann constant $\sigma = 5.67 \times 10^{-8} \mathrm{Wm^{-2}K^{-4}}$. The emission spectrum of the Sun is approximately that of a black body at temperature $T = 5800$ K.

(i) What is the total power emitted by the Sun?

(ii) Show that the solar radiation intensity reaching the surface of the Earth is approximately $1380\ \mathrm{Wm^{-2}}$. **Hint:** No knowledge of laser physics is needed.

(iii) Considering a standard laser pointer with a power of 1 mW, at what beam radius does the laser's intensity match that of the solar radiation on Earth?

(iv) Although the sun emits approximately a continuous range of frequencies (as a black body does), measurements of the solar spectrum on Earth reveals dark features today referred to as Franunhofer lines. Explain the physical origins of these lines.

Question 2: On resonators and mode-locking.

(a) Briefly explain what is meant with (i) the "longitudinal mode" and (ii) free-spectral range of an optical resonator.

(b) An optical resonator is formed by two mirrors separated by distance of $L = 2\ \mathrm{m}$. Assuming that the medium in between the mirrors is air, calculate the free-spectral range of the resonator.

(c) Briefly explain what is meant with "multimode" laser operation. Referring to the laser gain bandwidth and the resonator longitudinal modes, briefly explain how multimode operation can arise.

(d) Researchers at the University of Auckland have developed a mode-locked fibre laser whose cavity has a total round trip length of $L_{\mathrm{tot}} = 20\ \mathrm{m}$. The laser's gain bandwidth is found to be $\Delta f = 5\ \mathrm{THz}$, and the average power of the emitted laser beam is 100 mW. Assuming the refractive index of the fibre making the cavity is $n = 1.4$, answer the following questions:

(i) What is the free-spectral range of the cavity?

(ii) How many longitudinal modes is the laser emitting?

(iii) What is the temporal spacing between individual pulses?

(iv) What is the duration of the pulses generated through mode-locking?

(v) Give a rough estimate for the energy of individual pulses?

(vi) Give a rough estimate for the peak power of individual pulses?

Question 3: On frequency metrology.

(a) The ability to precisely measure unknown optical frequencies allows for the development of clocks that are more precise than current state-of-the-art atomic fountain clocks operating at radio frequencies (9.2 GHz). Briefly explain why.

(b) Briefly explain why precision measurements of unknown optical frequencies is difficult.

(c) Explain what is meant with "optical heterodyne detection".

(d) Two electromagnetic waves with equal amplitudes but different frequencies ω_1 and ω_2 are superimposed on a photodetector. Using the facts that (i) the waves can be written as $E_i(t) = E_0 \exp(\omega_i t)$ and (ii) the photodetector signal $i(t) \propto |E(t)|^2$, show that the photocurrent measured by the detector can be written as

$$i(t) = C(1 + \cos[(\omega_1 - \omega_2)t]), \tag{8.15}$$

where C is a constant.

(e) Explain what is meant with a "harmonic frequency chain".

(f) A scientist uses a precisely known reference electromagnetic wave with frequency $f_\mathrm{r} = 300$ THz to measure an unknown optical frequency f_u. A preliminary measurement has coarsely established that $f_\mathrm{u} > f_\mathrm{r}$. Figure 25 below shows the measured beat signal when the frequency comb line and the unknown optical wave are superimposed on a photodetector. Using the measured data, provide a more precise estimate for the value of the frequency f_u.

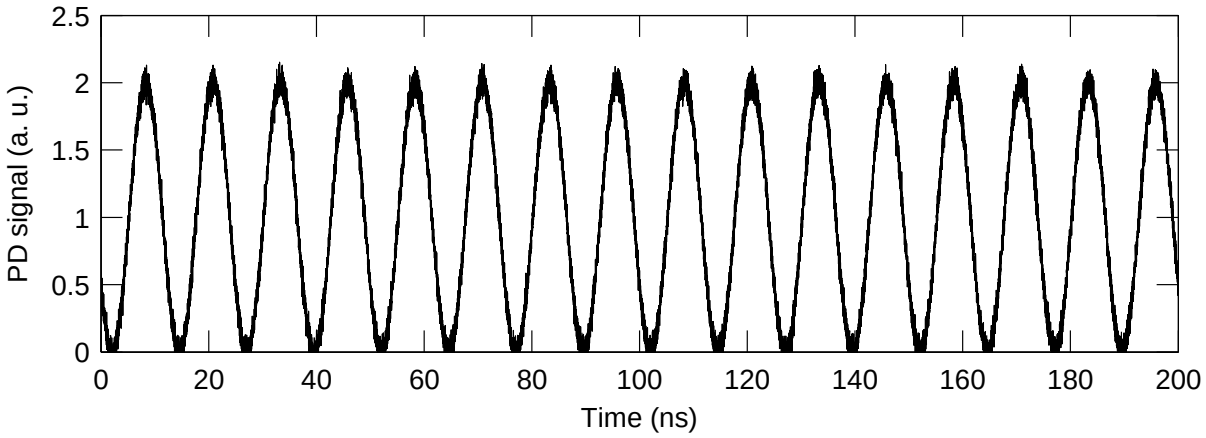

Figure 25: Beat signal measured on a photodetector (PD).

Question 4: On optical frequency combs.

(a) Explain what are optical frequency combs, how they are created, and how they can be used for precision measurements of unknown optical frequencies. A figure and/or an example might be helpful.

(b) The relationship $f_n = n f_{\mathrm{rep}} + f_{\mathrm{CEO}}$ is of particular significance for frequency combs. Define *each* of the terms, and describe its physical meaning.

(c) Figure 26 shows a pulse train emitted by a mode-locked Er:doped fibre laser as measured on a slow photodetector. What is the spacing of the individual spectral components of the optical frequency comb corresponding to the pulse train? Justify your answer.

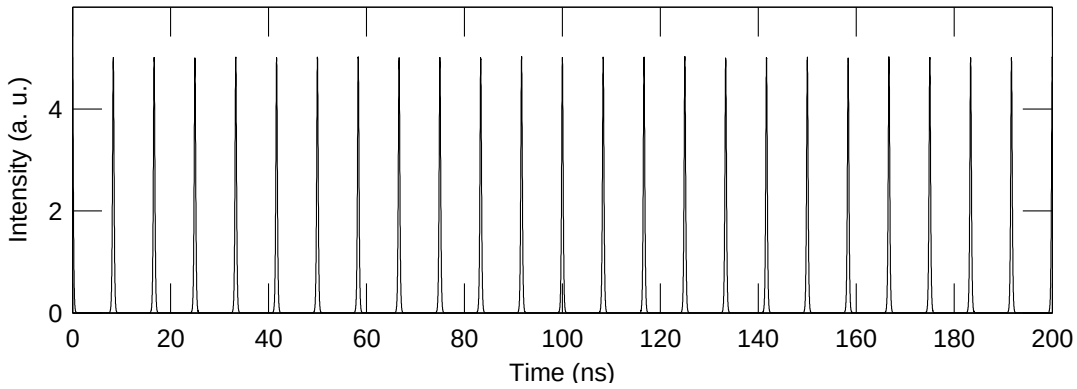

Figure 26: Pulse train measured on a photodetector.

(d) Explain the physical origins of the carrier-envelope offset phase, and describe how it affects the structure of mode-locked laser frequency combs. Furthermore, explain why the measurement shown in Fig. 26 does not yield any information of the carrier-envelope offset frequency.

(e) Explain what is meant with "referencing" in the context of optical frequency combs. Furthermore, provide brief descriptions of the following methods of referencing:

(i) Referencing with the help of a harmonic chain.

(ii) f-2f self-referencing.

Pictures are worth at least 20 words.

Question 5: On nonlinear optics

(a) Briefly explain what is meant with "second-harmonic generation" and cite at least one of its applications.

(b) Draw a schematic illustration of second-harmonic generation, clearly indicating the frequencies of the input and output beams.

(c) An optical parametric oscillator (OPO) is nonlinear optical device that can convert an input (pump) laser wave into two output waves of lower frequency. For historical reasons, the two output waves are known as "signal" and "idler", where the output wave with higher frequency is called signal. Consider an OPO pumped with an Nd:Yag laser (wavelength $\lambda = 1064\ \mathrm{nm}$). At the output, the signal wave is measured to have a wavelength of $\lambda_\mathrm{s} = 1410\ \mathrm{nm}$. What is the wavelength of the idler? **Hint:** energy conservation...

(d) How does the physical structure of a photonic crystal fibre differ from the structure of conventional step-index optical fibres?

(e) What is the role of photonic crystal fibres in the generation of self-referenced frequency combs? Why can we not use standard telecommunications single-mode fibres to do the same task?

(f) Figure 27 shows the group-velocity dispersion curves for two different photonic crystal fibres (PCF 1 and PCF 2). Which of the fibres is more ideal for the spectral broadening of pulses emitted by a Ti:Sapphire laser with a central wavelength of 800 nm? Justify your answer.

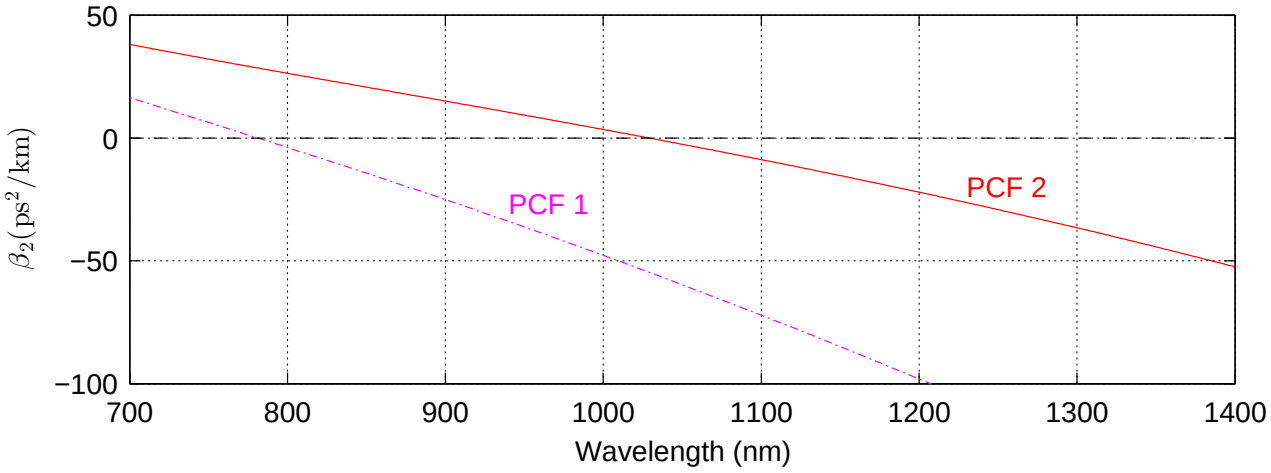

Figure 27: Group-velocity dispersion curves for PCF 1 (magenta dash-dotted) and PCF 2 (red solid curve).

Question 6: On microresonator frequency combs

(a) What are the advantageous characteristics of microresonator frequency combs compared to mode-locked laser frequency combs? Give an example of an application that could benefit from microresonator frequency combs.

(b) Explain why it is difficult to create optical frequency combs with a spacing in excess of 10 GHz using mode-locked lasers. Further explain how microresonators are more suitable for the job.

(c) In a recent study conducted at the University of Auckland[5], researchers investigated a silica microsphere resonator whose major diameter $d = 250\ \mu\mathrm{m}$. Calculate the resonator's free-spectral range. **Hint:** Consider the round trip length and remember that the refractive index of silica $n \approx 1.45$.

(d) To measure the finesse of the microsphere resonator, the researchers scanned the frequency of a tunable laser across a cavity resonance. From the measured signal, they inferred the resonance linewidth to be about $\Delta f \approx 5.2\ \mathrm{MHz}$. Calculate the finesse of the resonator.

(e) Calculate the value of the parameter ρ, and comment on the amount of power lost per round trip.

(f) In their experiments, the power of the driving field was set to $P_{\mathrm{in}} = 80\ \mathrm{mW}$. What is the intracavity power when the driving laser is exactly on-resonance? You can assume that the coupling is critical.

(g) Describe the fabrication process of one type of microresonator.

(h) Show that the steady-state intracavity power inside a coherently-driven passive resonator is given by the expression:

$$P_{\mathrm{in}}(\phi) = \frac{\theta P_{\mathrm{pump}}}{2 - \rho - 2\sqrt{1-\rho}\cos(\phi)}. \tag{8.16}$$

Derive this expression starting from the infinite-dimensional map described by Eq. 8.9 of the Lecture Notes.

(i) To measure the finesse of a resonator, it is customary to scan the pump laser frequency across several cavity resonances and measure the transmitted power as a function of frequency. This transmitted power corresponds to the superposition between the (1) "reflected" pump light that is not coupled into the resonator and (2) the part of the intracavity field that is coupled out of the resonator. As shown in Fig. 28, a typical signal consists of dips on a uniform background: the dips correspond to the cavity resonances. Using the data shown in Fig. 28, estimate the free-spectral range and finesse of the resonator.

[5] K. E. Webb et al., Opt. Lett. **41**, 4613 (2016)

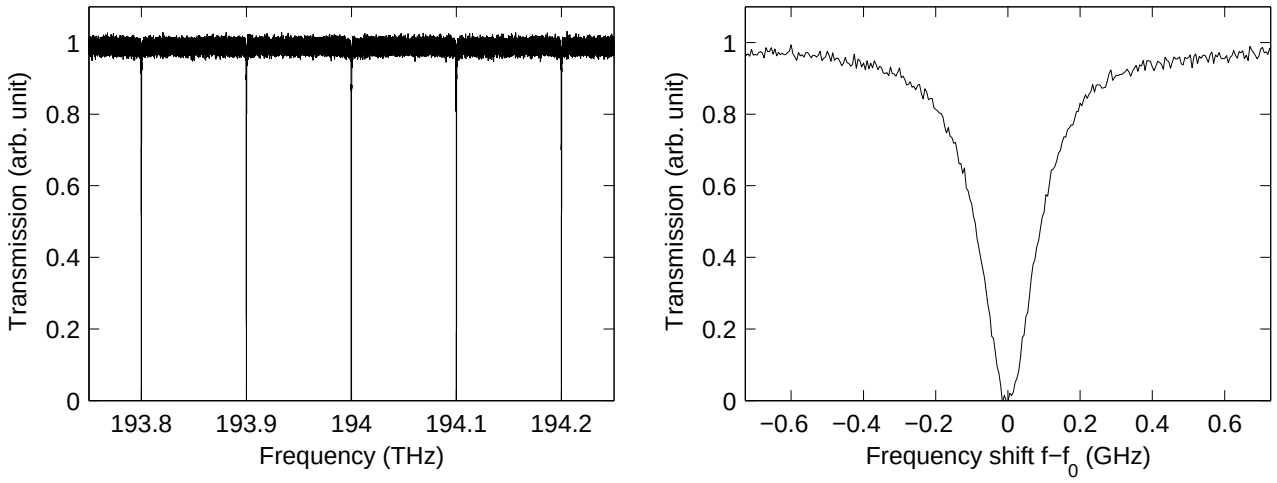

Figure 28: Measured transmission at the resonator output as a function of frequency. The right-panel shows a zoom on one of the resonances centred at $f_0 = 194$ THz.